Protection of double-Holliday junctions ensures crossing over during meiosis

Shangming Tang[1,2,3], Sara Hariri[1,2], Regina Bohn[1,2], John E, McCarthy[1,2], Jennifer Koo[1,2], Mohammad Pourhosseinzadeh[1,2], Emerald Nguyen[1,2], Natalie Liu[1,2], Christopher Ma[1,2], Hanyu Lu[1,2], Monica Lee[1,2], and Neil Hunter[1,2,4,*]

[1]Howard Hughes Medical Institute, University of California Davis, Davis, CA, USA.

[2]Department of Microbiology & Molecular Genetics, University of California Davis, Davis, CA, USA.

[3]Department of Biochemistry & Molecular Genetics, University of Virginia, Charlottesville, VA, USA.

[4]Department of Molecular & Cellular Biology, University of California, Davis, Davis, CA, USA.

*Correspondence to: Neil Hunter, E-mail: nhunter@ucdavis.edu

Chromosomal linkages formed through crossover recombination are essential for accurate segregation of homologous chromosomes during meiosis[1]. The DNA events of recombination are linked to structural components of meiotic chromosomes[2]. Imperatively, the biased resolution of double-Holliday junction intermediates (dHJs) into crossovers[3,4] occurs within the synaptonemal complex (SC), the meiosis-specific structure that mediates end-to-end synapsis of homologs during the pachytene stage[5,6]. However, the SC's roles in crossover-specific dHJ resolution remains unclear. Here, we show that key SC components function through dependent and interdependent relationships to protect dHJs from aberrant "dissolution" into noncrossover products. Conditional ablation experiments reveal that cohesin, the core of SC lateral elements, is required to maintain both synapsis and dHJ-associated crossover recombination complexes (CRCs) during pachytene. The SC central region transverse-filament protein is also required to maintain CRCs. Reciprocally, stability of the SC central region requires the continuous presence of CRCs, thereby coupling synapsis and desynapsis to dHJ formation and resolution. However, dHJ protection and maintenance of CRCs can occur without end-to-end homolog synapsis mediated by the central element of the SC central region. We conclude that local ensembles of SC components are sufficient to enable crossover-specific dHJ resolution and thereby ensure the linkage and segregation of homologous chromosomes.

46 During meiotic prophase I, cohesin complexes connect sister-chromatids and mediate their
47 organization into linear arrays of chromatin loops tethered to a common axis[2,5,7,8]. These cohesin-
48 based axes define interfaces for the pairing and synapsis of homologous chromosomes that
49 culminates in the formation of synaptonemal complexes (SCs), tripartite structures comprising
50 the two juxtaposed homolog axes, now called lateral elements, connected by a central lattice of
51 transverse filaments[5,6]. Extension of this lattice to achieve full synapsis requires an additional
52 central-element complex (see **Extended Data Fig. 1a**)[5,6,9]. Meiotic recombination facilitates
53 pairing and synapsis between homologous chromosomes, and then connects them via crossing
54 over, which is necessary for accurate segregation during the first meiotic division[1]. To this end,
55 the DNA events of recombination are physically and functionally linked to underlying
56 chromosome structures[2]. The protein complexes that catalyze DNA double-strand breaks (DSBs)
57 and subsequent strand exchange are tethered to homolog axes. Ensuing joint-molecule
58 intermediates and their associated recombination complexes interact with the SC central region.
59 A subset of recombination events is assigned a crossover fate with a tightly regulated
60 distribution, ensuring that each chromosome pair receives at least one[2]. At designated sites,
61 nascent joint molecules mature into double Holliday junctions (dHJs) and then undergo biased
62 resolution specifically into crossovers[3,4], all within the context of the SC central region and
63 associated crossover recombination complexes (CRCs). Post-synapsis roles of SC components in
64 crossing over remain unclear, particularly whether they function after dHJ formation to facilitate
65 crossover-specific resolution.
66
67 **Cohesin is required for crossover-biased dHJ resolution**

68 To address the role of SC lateral elements in crossover-specific dHJ resolution, the cohesin core
69 was ablated using the auxin-inducible degron (AID) system[10] to conditionally degrade Rec8 (the
70 meiosis-specific Kleisin subunit) at the time of dHJ resolution (**Fig. 1a**). Real-time inactivation
71 of Rec8-cohesin circumvents severe early meiotic defects of cohesin mutants in the formation
72 and processing of DSBs (**Extended Data Fig. 2a–d**)[11,12]. In all experiments, cell cultures were
73 synchronized at the resolution transition using an estradiol-inducible allele of *NDT80* (*NDT80-*
74 *IN*) that reversibly arrests cells at the pachytene stage, in which chromosomes are fully synapsed
75 and dHJs are poised for resolution[13].
76
77 Auxin and estradiol were added simultaneously to degrade Rec8-AID while releasing cells from
78 pachytene arrest and triggering dHJ resolution (**Fig. 1b–d**). Without auxin, Rec8-AID levels
79 remained high until cells had completed meiotic divisions (MI±MII); but with auxin, Rec8-AID
80 was completely degraded within 60 mins and meiotic divisions were delayed by ~2 hrs (**Fig. 1c**
81 and **1d**). Crossing over at the *HIS4::LEU2* DSB hotspot[14] was reduced by 70% following Rec8-
82 AID degradation, accompanied by a 43% increase in noncrossover products (**Fig. 1e–g**; note that
83 our assay reports a subset of noncrossover gene-conversion products, not absolute levels of
84 noncrossovers[14]). This reciprocal change in levels of crossover and noncrossover products, and
85 the comparable kinetics of their formation with and without auxin (**Fig. 1e,f**), suggest that dHJs
86 are efficiently resolved when Rec8-AID is degraded but their resolution fate is reversed. This
87 inference was confirmed by 2D-gel electrophoresis and Southern blotting (**Fig. 1h** and **1i**). Thus,
88 Rec8-based cohesin is required after dHJ formation to facilitate crossover-specific resolution.
89 Degradation of core cohesin subunit, Smc3, confirmed that the cohesin complex, not just Rec8,
90 is required (**Extended Data Fig. 2e–h**). However, the mitotic Kleisin, Mcd1[RAD21], is not required

91 for crossover-specific dHJ resolution indicating that this function is specific to Rec8-cohesin
92 (**Extended Data Fig. 2i,j**). We also showed that separase, Esp1, does not influence crossover-
93 specific resolution (**Extended Data Fig. 2i**), consistent with Yoon et al. [15] who showed that a
94 separase-resistant allele of Rec8 does not affect crossing over.
95
96 **Cohesin and Smc5/6 function in distinct resolution pathways**
97 Two classes of meiotic crossovers are distinguished by their dependencies on joint-molecule
98 resolving enzymes: class-I crossovers depend on the crossover-specific dHJ resolvase defined
99 by the endonuclease MutLγ (Mlh1-Mlh3)[3,4,16-18]; while minority class-II crossovers require
100 structure-selective endonucleases, primarily Mus81-Mms4^{Eme1} [3,19-21]. Epistasis analysis revealed
101 that cohesin and MutLγ act in the same crossover resolution pathway (**Fig. 2a,b**); while Mus81-
102 Mms4^{Eme1} acts in a parallel pathway (**Fig. 2c,d**, in these experiments Mms4-AID was degraded
103 at the resolution transition in a *yen1*Δ background in which backup resolvase Yen1 was deleted).
104 Crossover levels were indistinguishable following Rec8-AID degradation in the presence or
105 absence of MutLγ (*mlh3*Δ mutation; **Fig. 2b**). Noncrossover formation in *REC8-AID mlh3*Δ
106 strains was reduced to control levels suggesting that MutLγ influences whether products formed
107 in the absence of cohesin are associated with gene conversion of the SNP employed to detect
108 noncrossovers[14].
109
110 Mus81-Mms4^{Eme1} works in conjunction with a second SMC complex, Smc5/6 [20-23]. Consistently,
111 degradation of Nse4-AID (an essential subunit of Smc5/6) at the resolution transition reduced
112 crossing over to the same extent as when Mus81-Mms4^{Eme1} was inactivated by degrading Mms4-
113 AID (**Fig. 2c–f**). However, while noncrossovers were not reduced when Mus81-Mms4^{Eme1} was

114 inactivated, Nse4-AID degradation also reduced noncrossovers 2.1-fold (**Fig. 2e** and **2f**),
115 indicating that Smc5/6 controls an additional, Mus81-Mms4^{Eme1}-independent pathway of
116 noncrossover formation most likely by regulating a subpopulation of the Sgs1-Top3-Rmi1
117 complex (**Extended Data Figs. 1** and **3**).
118
119 Confirming that Smc5/6 and cohesin act in independent pathways of resolution, simultaneous
120 degradation of Nse4-AID and Smc3-AID resulted in an additive reduction in crossing over; and
121 noncrossover levels that are the combination of those observed when Nse4-AID and Smc3-AID
122 were degraded individually (**Fig. 2e** and **2f**; co-degradation of Nse4-AID and Rec8-AID gave
123 analogous results, **Extended Data Fig. 4**). Further distinguishing these two pathways, a subset of
124 joint molecules remained unresolved when Nse4-AID was degraded alone, while resolution
125 remained efficient when cohesin was inactivated (via degradation of either Rec8-AID or Smc3-
126 AID; **Figs. 1g,h** and **2g,h** and **Extended Data Fig. 4**); that is, Smc5/6 is essential for the
127 resolution of a subset of joint molecules into both crossovers and noncrossovers, while Rec8-
128 cohesin specifically promotes crossover-specific dHJ resolution, but is not required for resolution
129 *per se* (see **Extended Data Fig. 4c–f**).
130
131 **Rec8-cohesin is required to maintain synapsis and crossover recombination complexes**
132 **during pachytene**
133 To begin to understand how cohesin facilitates crossover-specific dHJ resolution, Rec8-AID was
134 degraded while pachytene arrest was maintained (no induction of *NDT80-IN*) and chromosomes
135 were analyzed by immunostaining for markers of homolog axes (Rec8 and Red1), SC central
136 region (Zip1), and crossover recombination complexes (CRCs; Msh5 and Zip3)[24](**Figure 3a**). In

137 no-auxin controls, linear Rec8 and discontinuous Red1 staining structures colocalized; and
138 synapsed homologs (indicated by lines of Zip1 staining) were decorated with foci of Msh5 and
139 Zip3 (**Fig. 3a**). One hour after auxin addition, Rec8 structures were lost and characteristic
140 features of pachytene chromosomes disappeared: SCs disassembled and Zip1 staining was now
141 confined to a few foci and larger structures resembling polycomplexes that are diagnostic of
142 defective synapsis; numbers of Red1 structures were reduced 2-fold, consistent with cohesins'
143 core function in organizing homolog axes[25] and directly recruiting Red1[26]; and CRCs dissociated
144 indicated by loss of Msh5 and Zip3 foci (**Fig. 3a** and **3b**). Thus, cohesin is required to maintain
145 the integrity of pachytene chromosome structures, consistent with analysis of meiotic cohesin in
146 *C. elegans*[27].
147
148 **Interdependent functions of the SC components are required for crossover-specific dHJ**
149 **resolution**
150 To discern which cohesin-dependent feature(s) of pachytene chromosomes is important for
151 crossover-specific dHJ resolution, SC transverse-filament protein Zip1[28,29] and pro-crossover
152 factor MutSγ were inactivated as cells were released from pachytene arrest (**Fig. 4a,b**). MutSγ (a
153 complex of Msh4 and Msh5) binds and stabilizes nascent joint molecules to promote homolog
154 synapsis and dHJ formation[30-32]. Both Zip1-AID and Msh4-AID degradation caused phenotypes
155 similar to those resulting from loss of cohesin, i.e. reduced crossovers and increased
156 noncrossovers (**Fig. 4c,d**), indicating continued roles after dHJs have formed to maintain their
157 crossover resolution fate.
158

159 This analysis suggests that cohesin may facilitate crossover-specific dHJ resolution by stabilizing
160 the SC central region, which in turn stabilizes CRCs. This interpretation was tested by
161 immunostaining the chromosomes of pachytene-arrested cells following degradation of Zip1-
162 AID (**Fig.4e,f**) or Msh4-AID (**Fig.4g,h**), respectively. When Zip1-AID was degraded, homologs
163 desynapsed but axis integrity was maintained as shown by robust Red1 localization (**Fig. 4e**). As
164 predicted, CRCs marked by Msh5 and Zip3 foci were diminished (**Fig. 4e,f**). As Zip3 and Msh4
165 protein levels remained high in these cells (**Extended Data Fig. 5**), we infer that CRCs are
166 disassembled when Zip1-AID is degraded. Unexpectedly, desynapsis occurred when Msh4-AID
167 was degraded revealing that the maintenance of SCs during pachytene requires the continued
168 presence of CRCs (**Fig. 4g**). Zip3 foci were also lost when Msh4-AID was degraded highlighting
169 the interdependence between Holliday-junction binding (MutSγ) and regulatory (Zip3)
170 components of CRCs (**Fig. 4g,h**).
171
172 **Pachytene chromosome structures protect dHJs from noncrossover resolution by the**
173 **Sgs1^{BLM}-Top3-Rmi1 complex**
174 dHJs normally remain stable in pachytene-arrested *NDT80-IN* cells because expression of polo-
175 like kinase Plk1^{Cdc5}, which activates dHJ resolution, requires the Ndt80 transcription factor [13,33].
176 However, dHJ levels decreased ~3-fold when Rec8-AID was degraded while maintaining
177 pachytene arrest (**Fig. 5b,c**) implying that pachytene chromosome structures protect dHJs from
178 aberrant resolution via a Plk1^{Cdc5}-independent resolution activity. A good candidate for this
179 activity is Sgs1^{BLM}-Top3-Rmi1 (STR), the budding yeast ortholog of human BLM complex
180 BLM-TOPIIIα-RMI1/2, and a robust decatenase enzyme that can "dissolve" dHJs specifically
181 into noncrossover products[34-38]. Confirming this prediction, dHJs were stabilized when Rec8-

182 AID and Top3-AID were simultaneously degraded (**Fig. 5a–c**; co-degrading Smc3-AID and
183 Top3-AID gave very similar results, **Extended Data Fig. 6**). Moreover, dHJ resolution
184 following Rec8-AID degradation alone produced noncrossover products that did not form when
185 Top3-AID was also degraded (**Fig. 5d,e**).
186
187 The stability of dHJs in pachytene-arrested cells following co-degradation of Rec8-AID and
188 Top3-AID indicates that resolution is once again dependent on $Plk1^{Cdc5}$ and suggests that the
189 crossover defect resulting from Rec8-AID degradation may be rescued. Indeed, expression of
190 *NDT80-IN* while simultaneously degrading Rec8-AID and Top3-AID resulted in a 2.6-fold
191 increase in crossovers relative to degradation of Rec8-AID alone, while noncrossovers decreased
192 1.6-fold (**Fig. 5f–h**; co-degradation of Rec8-AID and Sgs1-AID gave similar results, **Extended**
193 **Data Fig. 7**). Moreover, stabilization of dHJs and partial rescue of the crossover defects resulting
194 from Zip1-AID or Msh4-AID degradation were also seen when Top3-AID was simultaneously
195 degraded (**Extended Data Figs. 8** and **9**). Partial restoration of crossover levels is likely
196 explained by our observation that when STR function is ablated, essentially all resolution is
197 mediated by the Smc5/6–Mus81-Mms4 (**Extended Data Fig. 3**).
198
199 We wondered whether stabilizing dHJs also rescues the cytological defects resulting from
200 degradation of Rec8-AID, Zip1-AID, or Msh4-AID. To this end, Top3-AID was co-degraded
201 with Rec8-AID, Zip1-AID or Msh4-AID in pachytene-arrested cells, and chromosomes were
202 immunostained for markers of synapsis (Zip1), and CRCs (Msh4 and Zip3)(**Extended Data Fig.**
203 **10**). In each case, cytological phenotypes were largely indistinguishable from those observed
204 when Rec8-AID, Zip1-AID, or Msh4-AID were degraded alone. SCs and CRCs disassembled

205 following co-degradation of Rec8-AID and Top3-AID (**Extended Data Fig. 10a,b**); CRCs
206 dissociated when Zip1-AID and Top3-AID were co-degraded (**Extended Data Fig. 10c,d**); and
207 SCs disassembled following co-degradation of Msh4-AID and Top3-AID (**Extended Data Fig.**
208 **10e,f**). Thus, maintaining inter-homolog DNA connections by stabilizing dHJs does not bypass
209 the interdependencies between cohesin, SCs, and CRCs.
210
211 We conclude that the key components of pachytene chromosomes – cohesin-based homolog
212 axes, SC transverse filaments, and CRCs – protect crossover-designated dHJs from being
213 aberrantly dissolved into noncrossovers by the STR complex (see **Extended Data Fig. 1b**).
214
215 **Full synapsis is not essential for crossover-specific dHJ resolution**
216 High levels of crossing over can occur without end-to-end homolog synapsis in cells that lack the
217 SC central element, which is required to mature and extend the transverse filament lattice to
218 achieve full synapsis[5,6,9,39]. To determine whether maintenance of full synapsis is required for
219 crossover-specific dHJ resolution, central-element protein Ecm11[9] was ablated as cells were
220 released from pachytene arrest (**Fig. 6a,b**). Crossover and noncrossover levels were
221 indistinguishable from no-auxin controls when Ecm11-AID was degraded, sharply contrasting
222 phenotypes seen following loss of Rec8, Zip1, or Msh4 (**Figs. 1 and 4**). Moreover, in arrested
223 *NDT80-IN* cells, dHJs remained stable following Ecm11-AID degradation (**Fig. 6c,d**).
224
225 Immunostaining revealed that SCs disassembled following Ecm11-AID degradation in arrested
226 *NDT80-IN* cells, although numerous foci of Zip1 persisted (**Fig. 6e**). Thus, the central element is
227 required to both establish and maintain full synapsis. Msh5 and Zip3 foci were maintained at

228 ~50% of no-auxin control levels (**Fig. 6f,g**), in contrast to the almost complete loss seen
229 following degradation of Rec8-AID, Zip1-AID, or Msh4-AID. Moreover, remaining Msh5 and
230 Zip3 foci showed high degrees of colocalization with residual Zip1 structures (**Fig. 6h,i**). These
231 observations suggest that while mature SC may stabilize a subset of CRCs, local ensembles of
232 Zip1 and CRCs can be sufficient to protect dHJs and support crossover-specific resolution.
233

234 **Discussion**

235 The SC is an ancient structure that evolved with the emergence of sexual reproduction. Several
236 functions are attributed to the SC: assembly of homolog axes and pairwise synapsis of homologs
237 establish topological order in the nucleus; synapsis also attenuates formation of DSBs and
238 facilitates their repair, thereby diminishing DNA-damage checkpoint signaling; and at designated
239 crossover sites, SC components facilitate dHJ formation[5]. This study reveals that key SC
240 components, but not necessarily end-to-end synapsis *per se*, also enable crossover-specific
241 resolution of dHJs by protecting them from unscheduled dissolution into noncrossovers by the
242 conserved BLM/STR complex (**Extended Data Fig. 1b,c**). Failure of this critical final step of
243 meiotic recombination will result in unlinked univalent chromosomes that are prone to
244 missegregation, resulting in aneuploid gametes that are associated with infertility, miscarriage,
245 and congenital disease in humans.
246

247 Our data indicate that dHJs formed at crossover-designated recombination sites do not possess an
248 intrinsic structure or topology that constrains their resolution fate to ensure crossing over. We
249 previously proposed a model of crossover-specific resolution in which asymmetric loading of
250 PCNA during the DNA synthesis associated with dHJ formation subsequently directs strand-

251 specific nicking by the MutLγ endonuclease on both sides of the two Holliday junctions, but
252 distal to the exchange points[4]. This pattern of incisions always specifies a crossover outcome
253 when the nicked dHJs are disassembled by the BLM/STR complex. This two-step resolution
254 model reconciles the counterintuitive pro-crossover role of BLM/STR during meiosis, which
255 contradicts its well-characterized anti-crossover roles in unwinding D-loops and dissolving
256 unnicked dHJs into noncrossver products (**Extended Data Figs. 1b** and **3b,c**).
257
258 Within this framework, we propose that mature dHJs are unnicked and therefore vulnerable to
259 STR-catalyzed dissolution until MutLγ is activated via Ndt80-dependent expression of Plk1^{Cdc5}.
260 By preventing BLM/STR from acting on dHJs until they have been nicked by MutLγ, SC
261 components impose the sequential steps required for crossover-specific resolution (**Extended**
262 **Data Fig. 1b**).
263
264 We suggest that local ensembles of cohesin and SC transverse filaments can be sufficient protect
265 dHJs by stabilizing CRCs, components of which can directly bind HJs (including MutSγ, MutLγ,
266 Zip2^{SHOC1}-Spo16, and Mer3^{HFM1})[24,40] and may directly compete with BLM/STR for binding dHJs
267 and/or may constrain its activity. This suggestion is consistent with electron-microscopy
268 visualization of late recombination nodules associated with short patches of SC in *Sordaria*
269 *macrospora*[41]; and with the inference that, in *C. elegans,* the cohesin local to designated
270 crossover sites is distinctly regulated[27]. Moreover, components of the SC-central region help
271 recruit and stabilize CRCs [31,42-45]. Also in *C. elegans*, SC-central region proteins assemble
272 transient crossover-specific compartments or "bubbles" that may protect CRCs until crossover-
273 specific resolution is executed[43].

274

275 We also found that CRCs are required to maintain synapsis during pachytene. This observation is
276 consistent with studies indicating that the SC central region is initially dynamic and labile but
277 becomes more stable, contingent upon the development of CRCs[46-49]. Intriguingly, new subunits
278 are continually incorporated into the SC central region after synapsis[46,49]; and in budding yeast,
279 incorporation of new Zip1 molecules occurs predominantly at CRC sites[46]. Given that Zip1
280 appears to recruit CRC components directly[44,50], this suggests a possible mechanism for the
281 mutual stabilization of SCs and CRCs. This relationship may result in SCs with non-uniform
282 structure and stability[46], which could influence resolution fates and explain why sites of crossing
283 over are the last to desynpase during diplotene[51]. The interdependence and dynamicity of SCs
284 and CRCs will render chromosomal interactions readily reversible until dHJs are resolved into
285 crossovers. These attributes could help adjust and proof-read homologous synapsis, minimize
286 and resolve synaptic interlocks[52], and preserve genome stability by destabilizing interactions
287 between non-allelic and diverged sequences.

288

289 Importantly, dependency between synapsis and CRCs likely helps impose the ordered sequence
290 of events required to ensure crossing over between homologs. At designated crossover sites,
291 CRCs promote and maintain homolog synapsis, facilitate the formation of dHJs, and protect
292 them from aberrant dissolution. In turn, synapsis globally attenuates DSB formation[53],
293 diminishing the DNA-damage kinase signaling that inhibits Ndt80 activity. Ndt80-dependent
294 expression of Plk1^{Cdc5} then activates crossover-specific dHJ resolution, CRCs disassemble, and
295 desynapsis ensues (**Fig. 1c,d**)

296

297 Our analysis also reveals that two SMC complexes mediate essentially all Plk1^{Cdc5}-dependent
298 joint-molecule resolution during meiosis (**Extended Data Fig. 1c**). Rec8-cohesin is required to
299 maintain synapsis and CRCs, and thereby protects dHJs to facilitate crossover-specific dHJ
300 resolution. Whether local or global functions of Rec8-cohesin are important for crossover-
301 specific dHJ resolution, and the roles of cohesive versus chromatin-loop organizing populations
302 of Rec8-cohesin remain unclear. An independent Smc5/6 pathway is essential for resolution by
303 Mus81-Mms4^{EME1} and a subpopulation of BLM/STR, producing a mixture of crossovers and
304 noncrossovers. Despite these distinctions, Rec8-cohesin and Smc5/6 could have common
305 functions to constrain favorable joint-molecule topology[54] and control access by resolving
306 enzymes.
307
308 **References:**
309
310 1 Hunter, N. Meiotic Recombination: The Essence of Heredity. *Cold Spring Harbor*
311 *perspectives in biology* **7** (2015). https://doi.org/10.1101/cshperspect.a016618
312 2 Zickler, D. & Kleckner, N. Meiosis: Dances Between Homologs. *Annual review of*
313 *genetics* **57**, 1-63 (2023). https://doi.org/10.1146/annurev-genet-061323-044915
314 3 Zakharyevich, K., Tang, S., Ma, Y. & Hunter, N. Delineation of joint molecule resolution
315 pathways in meiosis identifies a crossover-specific resolvase. *Cell* **149**, 334-347 (2012).
316 https://doi.org/10.1016/j.cell.2012.03.023
317 4 Kulkarni, D. S. *et al.* PCNA activates the MutLgamma endonuclease to promote meiotic
318 crossing over. *Nature* (2020). https://doi.org/10.1038/s41586-020-2645-6

319 5 Zickler, D. & Kleckner, N. Recombination, pairing, and synapsis of homologs during
320 meiosis. *Cold Spring Harbor perspectives in biology* **7**, pii: a016626. doi:
321 016610.011101/cshperspect.a016626. (2015).
322 https://doi.org/10.1101/cshperspect.a016626
323 6 Adams, I. R. & Davies, O. R. Meiotic Chromosome Structure, the Synaptonemal
324 Complex, and Infertility. *Annu Rev Genomics Hum Genet* **24**, 35-61 (2023).
325 https://doi.org/10.1146/annurev-genom-110122-090239
326 7 Ito, M. & Shinohara, A. Chromosome architecture and homologous recombination in
327 meiosis. *Front Cell Dev Biol* **10**, 1097446 (2022).
328 https://doi.org/10.3389/fcell.2022.1097446
329 8 Schalbetter, S. A., Fudenberg, G., Baxter, J., Pollard, K. S. & Neale, M. J. Principles of
330 meiotic chromosome assembly revealed in S. cerevisiae. *Nature communications* **10**,
331 4795 (2019). https://doi.org/10.1038/s41467-019-12629-0
332 9 Humphryes, N. *et al.* The Ecm11-Gmc2 complex promotes synaptonemal complex
333 formation through assembly of transverse filaments in budding yeast. *PLoS genetics* **9**,
334 e1003194 (2013). https://doi.org/10.1371/journal.pgen.1003194
335 10 Nishimura, K., Fukagawa, T., Takisawa, H., Kakimoto, T. & Kanemaki, M. An auxin-
336 based degron system for the rapid depletion of proteins in nonplant cells. *Nature methods*
337 **6**, 917-922 (2009). https://doi.org/10.1038/nmeth.1401
338 11 Kugou, K. *et al.* Rec8 guides canonical Spo11 distribution along yeast meiotic
339 chromosomes. *Molecular biology of the cell* **20**, 3064-3076 (2009).
340 https://doi.org/10.1091/mbc.e08-12-1223

341 12 Kim, K. P. *et al.* Sister cohesion and structural axis components mediate homolog bias of
342 meiotic recombination. *Cell* **143**, 924-937 (2010).
343 https://doi.org/10.1016/j.cell.2010.11.015
344 13 Sourirajan, A. & Lichten, M. Polo-like kinase Cdc5 drives exit from pachytene during
345 budding yeast meiosis. *Genes & development* 22, 2627-2632 (2008).
346 https://doi.org/10.1101/gad.1711408
347 14 Owens, S., Tang, S. & Hunter, N. Monitoring Recombination During Meiosis in Budding
348 Yeast. *Methods Enzymol* **601**, 275-307 (2018).
349 https://doi.org/10.1016/bs.mie.2017.12.005
350 15 Yoon, S. W. *et al.* Meiotic prophase roles of Rec8 in crossover recombination and
351 chromosome structure. *Nucleic acids research* **44**, 9296-9314 (2016).
352 https://doi.org/10.1093/nar/gkw682
353 16 Cannavo, E. *et al.* Regulation of the MLH1-MLH3 endonuclease in meiosis. *Nature*
354 (2020). https://doi.org/10.1038/s41586-020-2592-2
355 17 Manhart, C. M. *et al.* The mismatch repair and meiotic recombination endonuclease
356 Mlh1-Mlh3 is activated by polymer formation and can cleave DNA substrates in trans.
357 *PLoS biology* **15**, e2001164 (2017). https://doi.org/10.1371/journal.pbio.2001164
358 18 Claeys Bouuaert, C. & Keeney, S. Distinct DNA-binding surfaces in the ATPase and
359 linker domains of MutLgamma determine its substrate specificities and exert separable
360 functions in meiotic recombination and mismatch repair. *PLoS genetics* **13**, e1006722
361 (2017). https://doi.org/10.1371/journal.pgen.1006722

362 19 De Los Santos, T. *et al.* The mus81/mms4 endonuclease acts independently of double-
363 holliday junction resolution to promote a distinct subset of crossovers during meiosis in
364 budding yeast. *Genetics* **164**, 81-94 (2003).
365 20 Copsey, A. *et al.* Smc5/6 coordinates formation and resolution of joint molecules with
366 chromosome morphology to ensure meiotic divisions. *PLoS genetics* **9**, e1004071 (2013).
367 https://doi.org/10.1371/journal.pgen.1004071
368 21 Xaver, M., Huang, L., Chen, D. & Klein, F. Smc5/6-mms21 prevents and eliminates
369 inappropriate recombination intermediates in meiosis. *PLoS genetics* **9**, e1004067 (2013).
370 https://doi.org/10.1371/journal.pgen.1004067
371 22 Wehrkamp-Richter, S., Hyppa, R. W., Prudden, J., Smith, G. R. & Boddy, M. N. Meiotic
372 DNA joint molecule resolution depends on Nse5-Nse6 of the Smc5-Smc6 holocomplex.
373 *Nucleic acids research* **40**, 9633-9646 (2012). https://doi.org/10.1093/nar/gks713
374 23 Peng, X. P. & Zhao, X. The multi-functional Smc5/6 complex in genome protection and
375 disease. *Nature structural & molecular biology* **30**, 724-734 (2023).
376 https://doi.org/10.1038/s41594-023-01015-6
377 24 Borner, G. V., Hochwagen, A. & MacQueen, A. J. Meiosis in budding yeast. *Genetics*
378 **225** (2023). https://doi.org/10.1093/genetics/iyad125
379 25 Sakuno, T. & Hiraoka, Y. Rec8 Cohesin: A Structural Platform for Shaping the Meiotic
380 Chromosomes. *Genes* **13** (2022). https://doi.org/10.3390/genes13020200
381 26 Sun, X. *et al.* Transcription dynamically patterns the meiotic chromosome-axis interface.
382 *eLife* **4** (2015). https://doi.org/10.7554/eLife.07424

383 27 Castellano-Pozo, M. *et al.* Surveillance of cohesin-supported chromosome structure
384 controls meiotic progression. *Nature communications* **11**, 4345 (2020).
385 https://doi.org/10.1038/s41467-020-18219-9
386 28 Tung, K. S. & Roeder, G. S. Meiotic chromosome morphology and behavior in zip1
387 mutants of Saccharomyces cerevisiae. *Genetics* **149**, 817-832 (1998).
388 29 Sym, M., Engebrecht, J. A. & Roeder, G. S. ZIP1 is a synaptonemal complex protein
389 required for meiotic chromosome synapsis. *Cell* **72**, 365-378 (1993).
390 30 Snowden, T., Acharya, S., Butz, C., Berardini, M. & Fishel, R. hMSH4-hMSH5
391 recognizes Holliday Junctions and forms a meiosis-specific sliding clamp that embraces
392 homologous chromosomes. *Molecular cell* **15**, 437-451 (2004).
393 31 He, W. *et al.* Regulated Proteolysis of MutSgamma Controls Meiotic Crossing Over.
394 *Molecular cell* **78**, 168-183 e165 (2020). https://doi.org/10.1016/j.molcel.2020.02.001
395 32 Borner, G. V., Kleckner, N. & Hunter, N. Crossover/noncrossover differentiation,
396 synaptonemal complex formation, and regulatory surveillance at the leptotene/zygotene
397 transition of meiosis. *Cell* **117**, 29-45 (2004).
398 33 Allers, T. & Lichten, M. Differential timing and control of noncrossover and crossover
399 recombination during meiosis. *Cell* **106**, 47-57 (2001).
400 34 Kaur, H., De Muyt, A. & Lichten, M. Top3-Rmi1 DNA single-strand decatenase is
401 integral to the formation and resolution of meiotic recombination intermediates.
402 *Molecular cell* **57**, 583-594 (2015). https://doi.org/10.1016/j.molcel.2015.01.020
403 35 Tang, S., Wu, M. K. Y., Zhang, R. & Hunter, N. Pervasive and essential roles of the
404 Top3-Rmi1 decatenase orchestrate recombination and facilitate chromosome segregation

405 in meiosis. *Molecular cell* **57**, 607-621 (2015).
406 https://doi.org/10.1016/j.molcel.2015.01.021
407 36 Fasching, C. L., Cejka, P., Kowalczykowski, S. C. & Heyer, W. D. Top3-Rmi1 dissolve
408 Rad51-mediated D loops by a topoisomerase-based mechanism. *Molecular cell* **57**, 595-
409 606 (2015). https://doi.org/10.1016/j.molcel.2015.01.022
410 37 Cejka, P., Plank, J. L., Bachrati, C. Z., Hickson, I. D. & Kowalczykowski, S. C. Rmi1
411 stimulates decatenation of double Holliday junctions during dissolution by Sgs1-Top3.
412 *Nature structural & molecular biology* **17**, 1377-1382 (2010).
413 https://doi.org/10.1038/nsmb.1919
414 38 Bythell-Douglas, R. & Deans, A. J. A Structural Guide to the Bloom Syndrome
415 Complex. *Structure* **29**, 99-113 (2021). https://doi.org/10.1016/j.str.2020.11.020
416 39 Voelkel-Meiman, K., Cheng, S. Y., Morehouse, S. J. & MacQueen, A. J. Synaptonemal
417 Complex Proteins of Budding Yeast Define Reciprocal Roles in MutSgamma-Mediated
418 Crossover Formation. *Genetics* **203**, 1091-1103 (2016).
419 https://doi.org/10.1534/genetics.115.182923
420 40 Pyatnitskaya, A., Borde, V. & De Muyt, A. Crossing and zipping: molecular duties of the
421 ZMM proteins in meiosis. *Chromosoma* **128**, 181-198 (2019).
422 https://doi.org/10.1007/s00412-019-00714-8
423 41 Zhang, L., Espagne, E., de Muyt, A., Zickler, D. & Kleckner, N. E. Interference-mediated
424 synaptonemal complex formation with embedded crossover designation. *Proceedings of*
425 *the National Academy of Sciences of the United States of America* **111**, E5059-5068
426 (2014). https://doi.org/10.1073/pnas.1416411111

427 42 Shinohara, M., Oh, S. D., Hunter, N. & Shinohara, A. Crossover assurance and crossover
428 interference are distinctly regulated by the ZMM proteins during yeast meiosis. *Nature*
429 *genetics* **40**, 299-309 (2008).
430 43 Woglar, A. & Villeneuve, A. M. Dynamic architecture of DNA repair complexes and the
431 synaptonemal complex at sites of meiotic recombination. *Cell* **173**, 1678-1691 e1616
432 (2018). https://doi.org/10.1016/j.cell.2018.03.066
433 44 Voelkel-Meiman, K. *et al.* Crossover recombination and synapsis are linked by adjacent
434 regions within the N terminus of the Zip1 synaptonemal complex protein. *PLoS genetics*
435 **15**, e1008201 (2019). https://doi.org/10.1371/journal.pgen.1008201
436 45 Cahoon, C. K., Helm, J. M. & Libuda, D. E. Synaptonemal Complex Central Region
437 Proteins Promote Localization of Pro-crossover Factors to Recombination Events During
438 Caenorhabditis elegans Meiosis. *Genetics* **213**, 395-409 (2019).
439 https://doi.org/10.1534/genetics.119.302625
440 46 Voelkel-Meiman, K., Moustafa, S. S., Lefrancois, P., Villeneuve, A. M. & MacQueen, A.
441 J. Full-length synaptonemal complex grows continuously during meiotic prophase in
442 budding yeast. *PLoS genetics* **8**, e1002993 (2012).
443 https://doi.org/10.1371/journal.pgen.1002993
444 47 Rog, O., Kohler, S. & Dernburg, A. F. The synaptonemal complex has liquid crystalline
445 properties and spatially regulates meiotic recombination factors. *eLife* **6** (2017).
446 https://doi.org/10.7554/eLife.21455
447 48 Nadarajan, S. *et al.* Polo-like kinase-dependent phosphorylation of the synaptonemal
448 complex protein SYP-4 regulates double-strand break formation through a negative
449 feedback loop. *eLife* **6** (2017). https://doi.org/10.7554/eLife.23437

450 49 Pattabiraman, D., Roelens, B., Woglar, A. & Villeneuve, A. M. Meiotic recombination
451 modulates the structure and dynamics of the synaptonemal complex during C. elegans
452 meiosis. *PLoS genetics* **13**, e1006670 (2017).
453 https://doi.org/10.1371/journal.pgen.1006670
454 50 Agarwal, S. & Roeder, G. S. Zip3 provides a link between recombination enzymes and
455 synaptonemal complex proteins. *Cell* **102**, 245-255 (2000).
456 51 Qiao, H. *et al.* Interplay between synaptonemal complex, homologous recombination,
457 and centromeres during mammalian meiosis. *PLoS genetics* **8**, e1002790 (2012).
458 https://doi.org/10.1371/journal.pgen.1002790
459 52 Olaya, I., Burgess, S. M. & Rog, O. Formation and resolution of meiotic chromosome
460 entanglements and interlocks. *Journal of cell science* **137** (2024).
461 https://doi.org/10.1242/jcs.262004
462 53 Mu, X., Murakami, H., Mohibullah, N. & Keeney, S. Chromosome-autonomous feedback
463 down-regulates meiotic DNA break competence upon synaptonemal complex formation.
464 *Genes & development* **34**, 1605-1618 (2020). https://doi.org/10.1101/gad.342873.120
465 54 Roy, S., Adhikary, H. & D'Amours, D. The SMC5/6 complex: folding chromosomes
466 back into shape when genomes take a break. *Nucleic acids research* **52**, 2112-2129
467 (2024). https://doi.org/10.1093/nar/gkae103
468
469

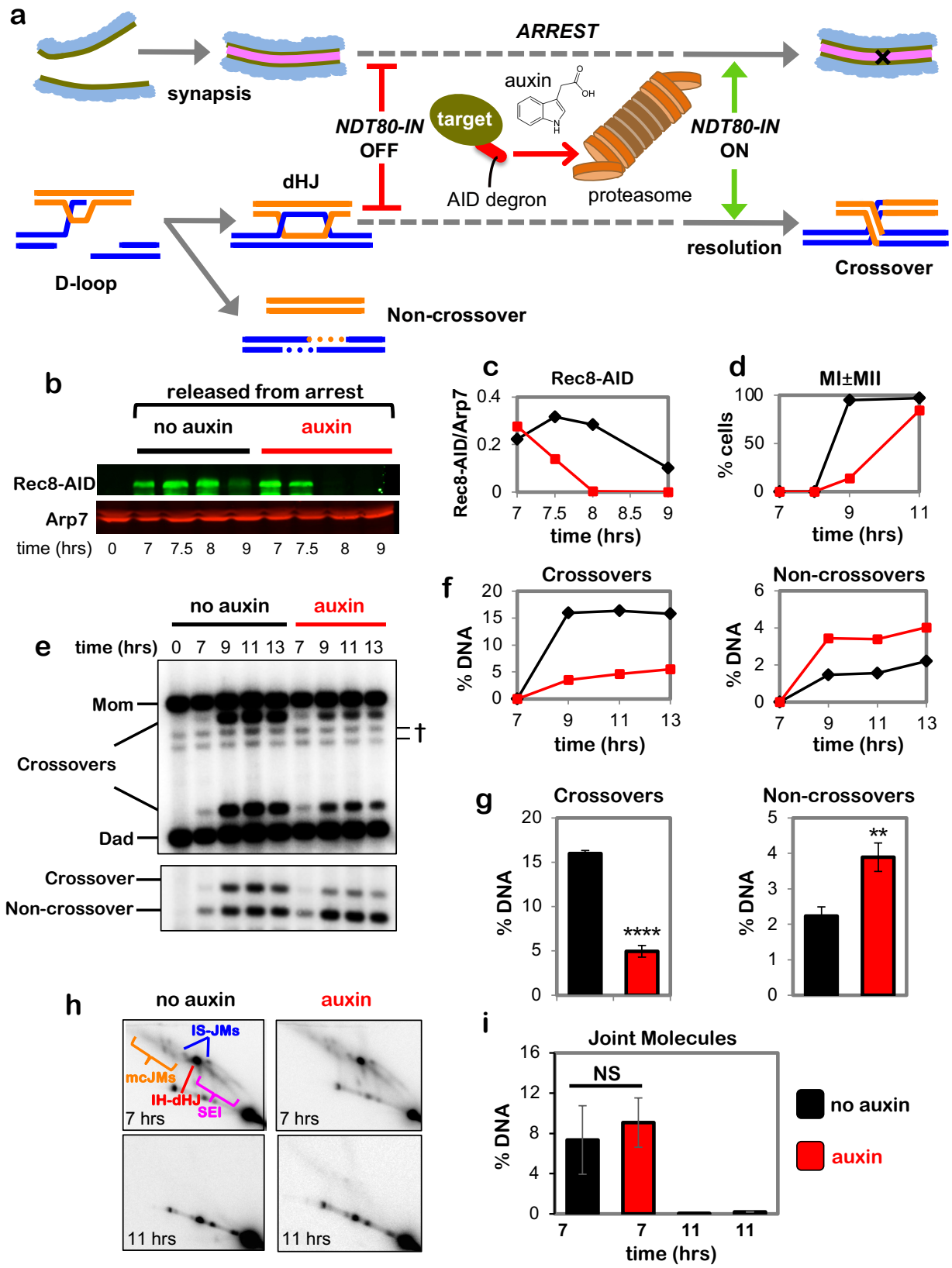
a
synapsis
ARREST
NDT80-IN
OFF
target
auxin
NDT80-IN
ON
dHJ
AID degron
proteasome
D-loop
resolution
Crossover
Non-crossover
b
released from arrest
no auxin
auxin
Rec8-AID
Arp7
time (hrs) 0 7 7.5 8 9 7 7.5 8 9
c
Rec8-AID
Rec8-AID/Arp7
time (hrs)
d
MI±MII
% cells
time (hrs)
e
no auxin
auxin
time (hrs) 0 7 9 11 13 7 9 11 13
Mom
Crossovers
Dad
Crossover
Non-crossover
f
Crossovers
Non-crossovers
% DNA
time (hrs)
g
Crossovers
Non-crossovers
% DNA
****
**
h
no auxin
auxin
IS~JMs
mcJMs
IH-dHJ
SEI
7 hrs
11 hrs
i
Joint Molecules
NS
% DNA
time (hrs)
no auxin
auxin

470

471 **Fig. 1. Rec8-cohesin is required for crossover-specific dHJ resolution.**

472 **a,** Experimental strategy. Top row: homolog synapsis with chromatin in blue, green homolog
473 axes, and pink SC central region. The **X** in the final cartoon indicates a crossover formed after
474 Ndt80 is expressed. Middle row: cell synchronization at the dHJ resolution transition using the
475 inducible *NDT80-IN* allele; and conditional degradation of target proteins using the AID system.
476 Bottom row: DNA events of meiotic recombination. Only the two chromosomes engaged in
477 recombination are shown.

478 **b,** Western analysis of Rec8-AID from subcultures with or without the addition of auxin at 7
479 hours. Arp7 is used as a loading control.

480 **c,** Quantification of Rec8-AID level from the experiment shown in panel **b**.

481 **d,** Quantification of nuclear divisions (MI±MII, cells with two and four nuclei) from *REC8-AID*
482 subcultures with or without auxin.

483 **e,** Representative 1D-gel Southern analysis of crossover (upper panel) and non-crossover (lower
484 panel) formation at the *HIS4::LEU2* recombination hotspot from *REC8-AID* subcultures with or
485 without auxin. † cross-hybridizing background bands.

486 **f,** Quantification of crossovers and non-crossovers levels from the experiments shown in panel **e**.

487 **g,** Quantification of final levels of crossovers and non-crossovers at 11 hrs from *REC8-AID*
488 subcultures with or without auxin (mean ± SD, 3 independent experiments, ****P<0.0001,
489 **P=0.0038. two-tailed unpaired t-test).

490 **h,** Representative 2D gel Southern analysis of joint molecules from *REC8-AID* subcultures with
491 or without auxin, before and after release from arrest at 7 and 11 hrs, respectively. The upper left
492 panel highlights joint-molecule species: SEI, single end invasion; IH-dHJ, inter-homolog double

493 Holliday junction; IS-JMs, inter-sister joint molecules; mc-JMs, 3- and 4-chromatid joint

494 molecules.

495 **i,** Quantification of total joint molecule levels from experiments represented in panel **h** (mean ±

496 SD, n=3 independent experiments, NS, not significant, P=0.4561, two-tailed unpaired t-test).

497

498

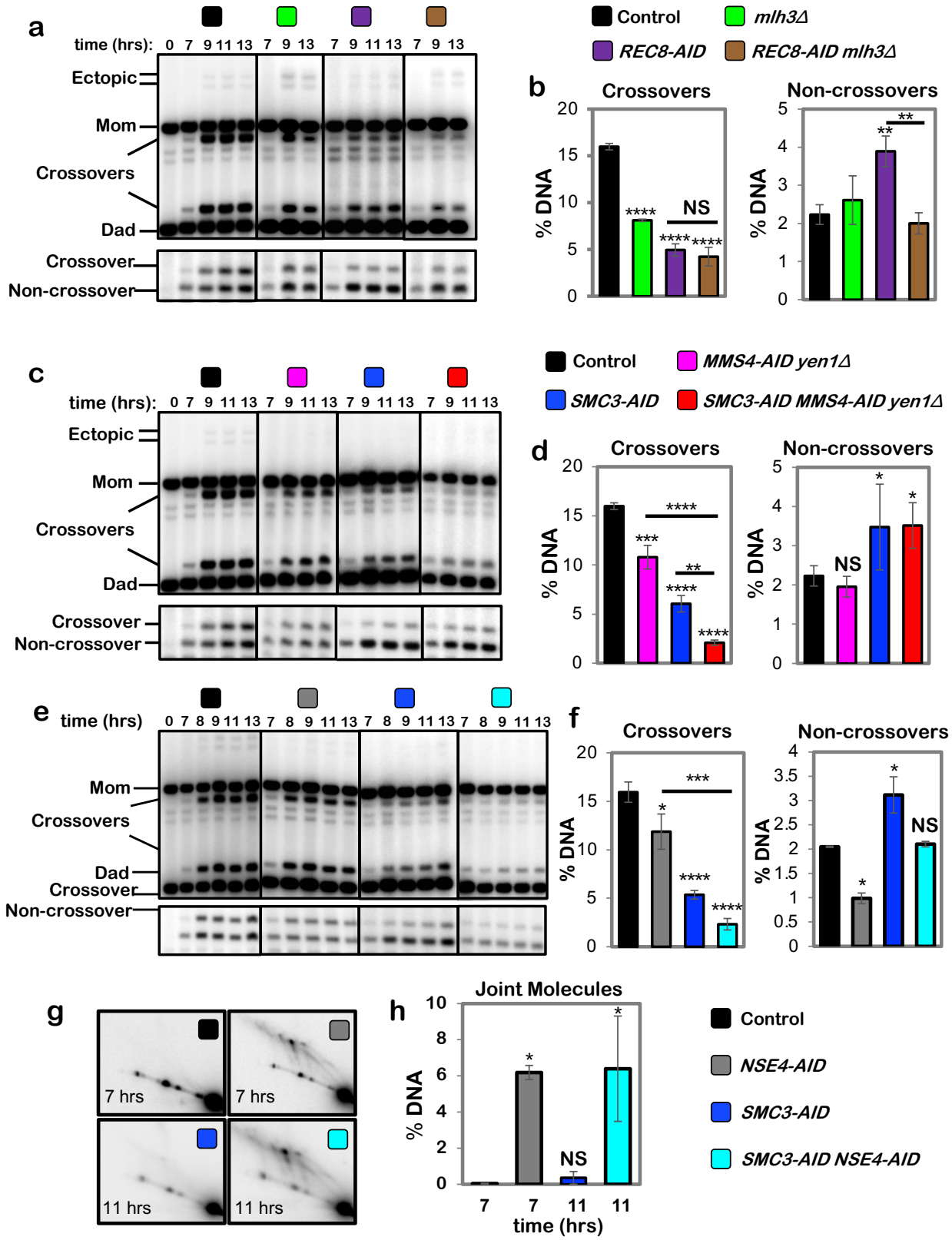
a
time (hrs): 0 7 9 11 13 7 9 13 7 9 11 13 7 9 13
Ectopic
Mom
Crossovers
Dad
Crossover
Non-crossover
Control
mlh3Δ
REC8-AID
REC8-AID mlh3Δ
b
Crossovers
Non-crossovers
% DNA
NS
c
time (hrs): 0 7 9 11 13 7 9 11 13 7 9 11 13 7 9 11 13
Control
MMS4-AID yen1Δ
SMC3-AID
SMC3-AID MMS4-AID yen1Δ
d
e
time (hrs) 0 7 8 9 11 13 7 8 9 11 13 7 8 9 11 13 7 8 9 11 13
f
g
7 hrs
11 hrs
h
Joint Molecules
time (hrs)
NSE4-AID
SMC3-AID NSE4-AID

499

500 **Fig. 2. Rec8-cohesin and Smc5/6 define distinct pathways of joint-molecule resolution.**

501 In all experiments, cells were released from *NDT80-IN* arrest.

502 **a,** Representative 1D-gel Southern analysis of crossover (upper panel) and non-crossover (lower

503 panel) formation in control (*REC8-AID* no auxin), *mlh3*Δ, *REC8-AID* (with auxin) and *REC8-*

504 *AID mlh3*Δ (with auxin) strains.

505 **b,** Final levels of crossovers and non-crossovers at 13 hrs from the indicated strains (mean ± SD,

506 3 independent experiments). Statistical comparisons with control unless indicated. Dunnett's

507 multiple comparisons test, ****P<0.0001, NS, not significant P=0.5281, **P=0.0034 (*REC8-*

508 *AID* vs. control), **P=0.0026 (*REC8-AID* vs. *REC8-AID mlh3*Δ).

509 **c,** Representative 1D-gel Southern analysis of crossover (upper panel) and non-crossover (lower

510 panel) formation in control, *MMS4-AID yen1*Δ (with auxin), *SMC3-AID* (with auxin) and *SMC3-*

511 *AID MMS4-AID yen1*Δ (with auxin) strains.

512 **d,** Final levels of crossovers and non-crossovers at 11 hrs from the indicated strains (mean ± SD,

513 3 independent experiments. Statistical comparisons with control unless indicated. For crossovers,

514 Tukey's multiple comparisons test was performed; for non-crossovers, Dunnett's multiple

515 comparisons test was performed. ****P<0.0001, ***P=0.0003, **P=0.0066, *P= 0.0385

516 (control vs. *SMC3-AID*), *P=0.0488 (control vs. *SMC3-AID MMS4-AID yen1*Δ.), NS, not

517 significant P=0.7806).

518 **e,** Representative 1D-gel Southern analysis of crossover (upper panel) and non-crossover (lower

519 panel) formation in control, *NSE4-AID* (with auxin), *REC8-AID* (with auxin) and *REC8-AID*

520 *NSE4-AID* (with auxin) strains.

521 **f,** Final levels of crossovers and non-crossovers at 11 hrs from the indicated strains (mean ± SD,

522 3 independent experiments). Statistical comparisons with control unless indicated. For

523 crossovers, Tukey's multiple comparisons test was performed; for non-crossovers, Dunnett's
524 multiple comparisons test was performed. ****P<0.0001, ***P=0.0003, *P= 0.0262 (control vs,
525 *NSE4-AID* for crossover comparison), *P= 0.0464 (control vs. SMC3-AID for non-crossover
526 comparison), NS, not significant, P=0.1148 (control vs. *NSE4-AID*), P >0.9999 (control vs.
527 *SMC3-AID NSE4-AID*).
528 **g,** Representative 2D gel Southern analysis of joint molecules from control, *NSE4-AID* (with
529 auxin), *SMC3-AID* (with auxin) and *SMC3-AID NSE4-AID* (with auxin) strains.
530 **h,** Quantification of total joint-molecule levels from the indicated strains. (mean ± SD, 3
531 independent experiments). Dunnett's multiple comparisons test with control: *P=0.0164 (control
532 vs. *NSE4-AID*), *P=0.0097 (control vs. *SMC3-AID NSE4-AID*, NS, not significant, P=0.9954).
533

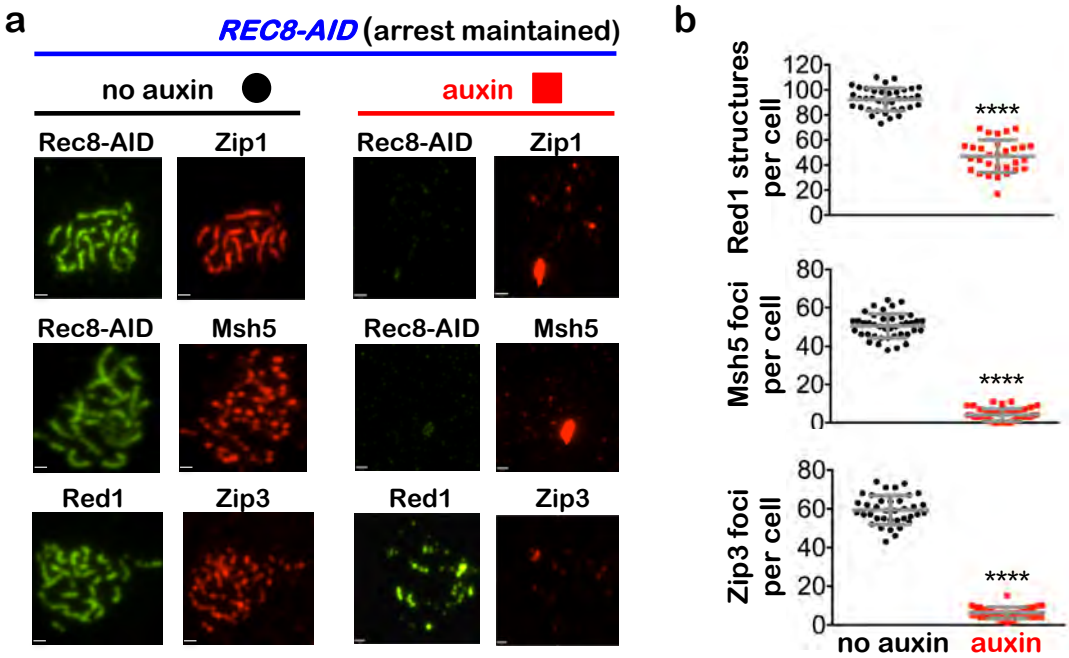

534

535

536 **Fig. 3. Rec8-cohesin is required to maintain synaptonemal complexes and crossover-**

537 **specific recombination complexes.**

538 **a,** Representative images of surface-spread meiotic nuclei from *REC8-AID* cultures in which

539 pachytene-arrest was maintained. Cells were sampled 1 hr after the addition of auxin or DMSO

540 vehicle at 7 hrs, and immunostained for the indicated markers. Scale bars = 1 μm.

541 **b,** Quantification of Red1, Msh5 and Zip3 immunostaining structures from experiments

542 represented in **a**. 40-60 nuclei were counted in each case. Error bars represent SD. Unpaired two-

543 tailed *t* test. ****$P<0.0001$.

544

545

546

547

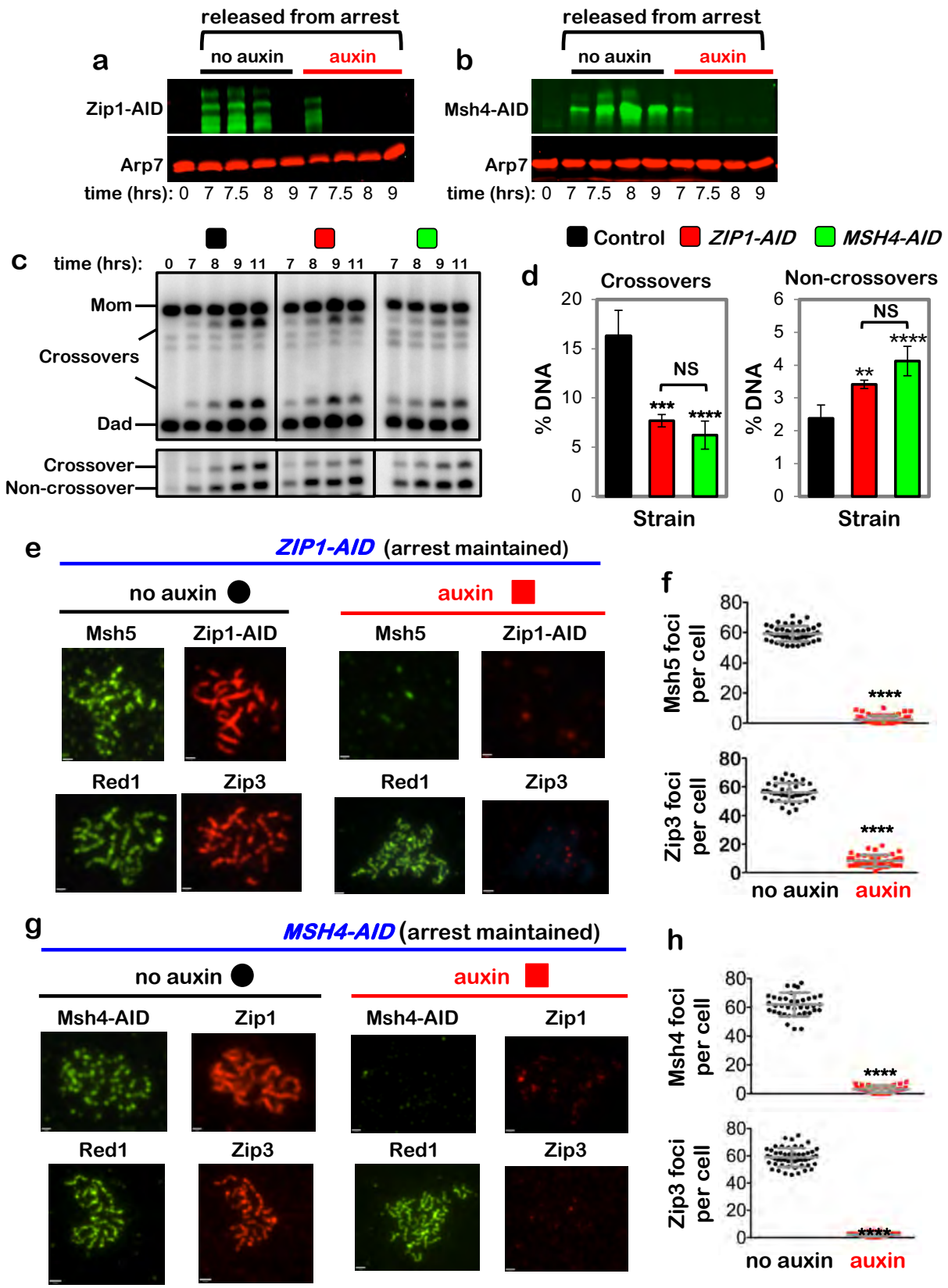
a
released from arrest
no auxin
auxin
Zip1-AID
Arp7
time (hrs): 0 7 7.5 8 9 7 7.5 8 9
b
released from arrest
no auxin
auxin
Msh4-AID
Arp7
time (hrs): 0 7 7.5 8 9 7 7.5 8 9
c
time (hrs): 0 7 8 9 11 7 8 9 11 7 8 9 11
Mom
Crossovers
Dad
Crossover
Non-crossover
Control
ZIP1-AID
MSH4-AID
d
Crossovers
Non-crossovers
% DNA
NS
***
****
**
Strain
e
ZIP1-AID (arrest maintained)
no auxin
auxin
Msh5
Zip1-AID
Red1
Zip3
f
Msh5 foci per cell
Zip3 foci per cell
****
no auxin
auxin
g
MSH4-AID (arrest maintained)
no auxin
auxin
Msh4-AID
Zip1
Red1
Zip3
h
Msh4 foci per cell
Zip3 foci per cell
****
no auxin
auxin

548

549 **Figure 4. Zip1 and MutSγ are required for crossover-specific dHJ resolution**

550 **a,** Western blot analysis of Zip1-AID from subcultures with or without the addition of auxin at 7
551 hours. Arp7 is a loading control.

552 **b,** Western blot analysis of Msh4-AID from subcultures with or without the addition of auxin at
553 7 hours. Arp7 is used as a loading control.

554 **c,** Representative 1D-gel Southern analysis of crossover (upper panel) and non-crossover (lower
555 panel) formation in control, *ZIP1-AID* (with auxin) and *MSH4-AID* (with auxin) strains.

556 **d,** Final levels of crossovers and non-crossovers at 11 hrs from the indicated strains.
557 Error bars represent SD for three independent experiments. Statistical comparisons with control
558 unless indicated. Tukey's multiple comparisons test, ****$P<0.0001$, **$P=0.0099$, NS, not
559 significant, $P=0.3353$ (*ZIP1-AID* vs. *MSH4-AID* for crossover analysis), $P=0.0763$ (*ZIP1-AID*
560 vs. *MSH4-AID* for non-crossover analysis).

561 **e,** Representative images of surface-spread meiotic nuclei from pachytene-arrested *ZIP1-AID*
562 cells sampled 1 hr after the addition of auxin or DMSO vehicle at 7 hrs, and immunostained for
563 the indicated markers. Scale bars = 1 μm.

564 **f,** Quantification of Msh5 and Zip3 immunostaining foci from the experiments represented in
565 panel **e**. 40-60 nuclei were counted in each case. Error bars represent SD. Unpaired two-tailed *t*
566 test, $P<0.0001$.

567 **g,** Representative images of surface-spread meiotic nuclei from pachytene-arrested *MSH4-AID*
568 cells sampled 1 hr after the addition of auxin or DMSO vehicle at 7 hrs, and immunostained for
569 the indicated markers.

570 **h,** Quantification of Msh4 and Zip3 immunostaining foci from the experiments represented in

571 panel **g**. 40-60 nuclei were counted in each case. Error bars represent SD. 40-60 nuclei were

572 counting for each set of data.

573 In **e** and **g**, scale bars = 1 μm. Unpaired two-tailed *t* test, ****$P<0.0001$.

574

575

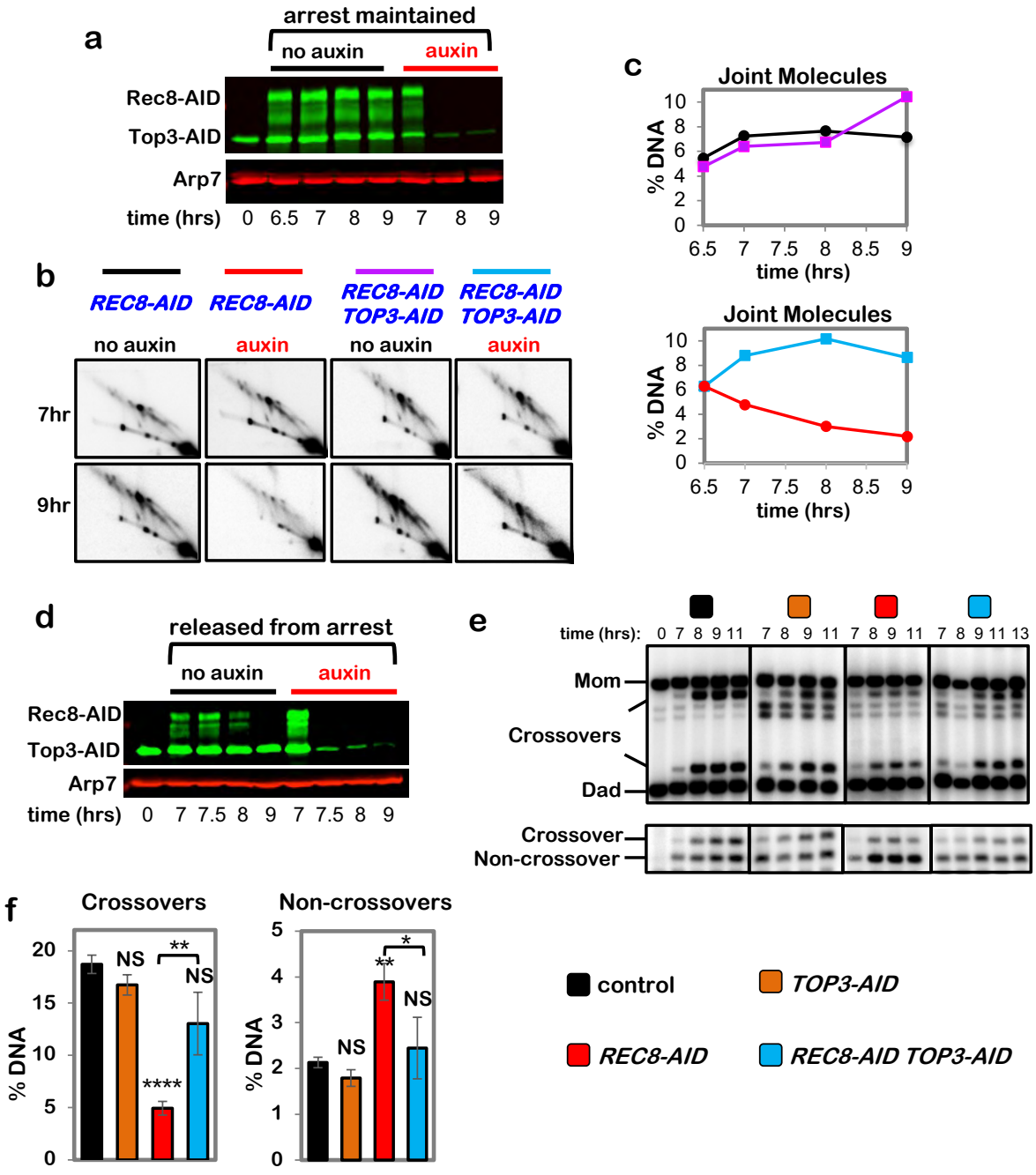
a
arrest maintained
no auxin
auxin
Rec8-AID
Top3-AID
Arp7
time (hrs) 0 6.5 7 8 9 7 8 9
b
REC8-AID
REC8-AID
REC8-AID TOP3-AID
REC8-AID TOP3-AID
no auxin
auxin
no auxin
auxin
7hr
9hr
c
Joint Molecules
% DNA
time (hrs)
Joint Molecules
% DNA
time (hrs)
d
released from arrest
no auxin
auxin
Rec8-AID
Top3-AID
Arp7
time (hrs) 0 7 7.5 8 9 7 7.5 8 9
e
time (hrs): 0 7 8 9 11 7 8 9 11 7 8 9 11 7 8 9 11 13
Mom
Crossovers
Dad
Crossover
Non-crossover
f
Crossovers
Non-crossovers
% DNA
NS
**
NS
****
*
**
NS
NS
control
TOP3-AID
REC8-AID
REC8-AID TOP3-AID

576

577 **Fig, 5. Rec8-cohesin protects double-Holliday junctions from aberrant resolution mediated**
578 **by the BLM/STR complex.**
579 **a,** Western blot analysis of Top3-AID and Rec8-AID from subcultures with or without the
580 addition of auxin at 7 hours while maintaining pachytene arrest. Arp7 is a loading control. The
581 degradation-resistant fraction of Top3-AID is mitochondrial.
582 **b,** Representative 2D gel Southern analysis of joint molecules from *REC8-AID* and *REC8-AID*
583 *TOP3-AID* strains with and without the addition of auxin.
584 **c,** Quantification of total joint molecule levels from the indicated strains.
585 **d,** Western blot analysis of Top3-AID and Rec8-AID from subcultures with or without the
586 addition of auxin at 7 hours with release from pachytene arrest.
587 **e,** Representative 1D-gel Southern analysis of crossover (upper panel) and non-crossover (lower
588 panel) formation in control, *TOP3-AID* (with auxin), *REC8-AID* (with auxin) and *REC8-AID*
589 *TOP3-AID* (with auxin) strains.
590 **f,** Final levels of crossovers and non-crossovers at 11 hrs from experiments represented in **g**.
591 Error bars represent SD for three independent experiments. Statistical comparisons with control
592 unless indicated. Tukey's multiple comparisons test, ****P<0.0001, **P=0.0011 (*REC8-AID* vs.
593 *REC8-AID TOP3-AID* for crossover comparison), NS, not significant, P=0.8881 (control vs.
594 *TOP3-AID* for crossover comparison), NS, not significant, P=0.0.1516 (control vs. *REC8-AID*
595 *TOP3-AID* for crossover comparison), **P=0.0041 (control vs. REC8-AID for non-crossover
596 comparison), *P=0.0156, NS, not significant, P=0.5131 (control vs. *TOP3-AID* for non-
597 crossover comparison), P= 0.9200 (control vs. *REC8-AID TOP3-AID* for non-crossover
598 comparison).
599

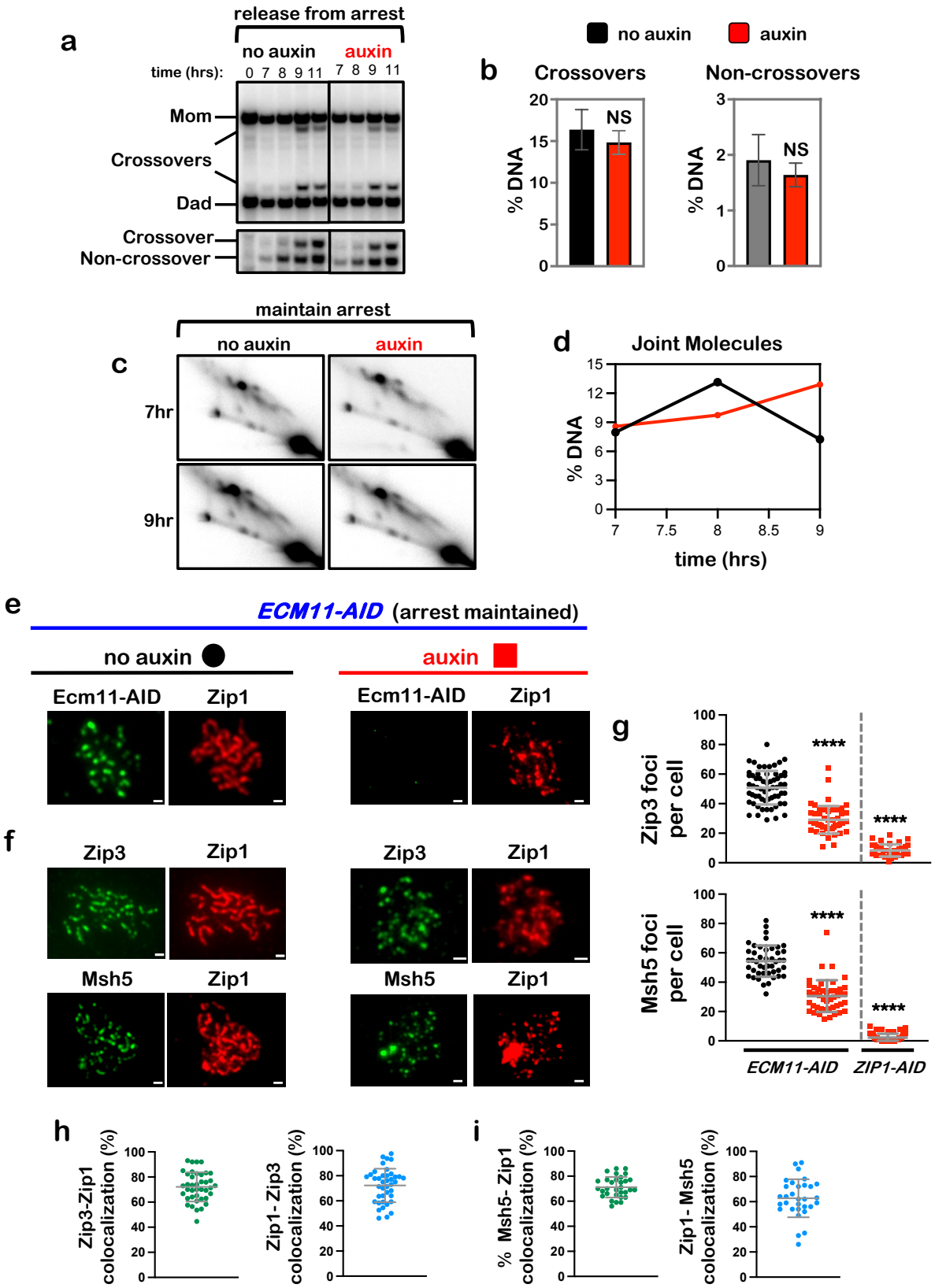
a
release from arrest
no auxin
auxin
time (hrs):
0 7 8 9 11
7 8 9 11
Mom
Crossovers
Dad
Crossover
Non-crossover
b
no auxin
auxin
Crossovers
Non-crossovers
% DNA
NS
NS
c
maintain arrest
no auxin
auxin
7hr
9hr
d
Joint Molecules
% DNA
time (hrs)
e
ECM11-AID (arrest maintained)
no auxin
auxin
Ecm11-AID
Zip1
f
Zip3
Msh5
g
Zip3 foci per cell
Msh5 foci per cell
****
ECM11-AID
ZIP1-AID
h
Zip3-Zip1 colocalization (%)
Zip1- Zip3 colocalization (%)
i
% Msh5- Zip1 colocalization (%)
Zip1- Msh5 colocalization (%)

600

601 **Fig. 6. Full synapsis is not essential for crossover-specific dHJ resolution.**

602 **a,** Representative 1D-gel Southern analysis of crossover (upper panel) and non-crossover (lower
603 panel) formation from *ECM11-AID* subcultures with or without auxin. NS, not significant,
604 unpaired two-tailed *t*-test.

605 **b,** Final levels of crossovers and non-crossovers at 11 hrs from the experiments represented in
606 panel **a**. Error bars represent SD for three independent experiments.

607 **c**, Representative 2D gel Southern analysis of joint molecules from *ECM11-AID* subcultures
608 with and without the addition of auxin while maintaining pachytene arrest.

609 **d,** Quantification of total joint molecule levels from experiment represented in panel **c**.

610 **e, f,** Representative images of surface-spread meiotic nuclei from pachytene-arrested *ECM11-*
611 *AID* cells sampled 1 hr after the addition of auxin or DMSO vehicle at 7 hrs, and immunostained
612 for the indicated markers. Scale bars = 1 μm.

613 **g,** Quantification of Zip3 and Msh5 immunostaining foci from the *ECM11-AID* experiments
614 represented in panels **e** and **f**, and comparison with corresponding data from *ZIP1-AID* (from
615 **Fig. 4f**). 40-60 nuclei were counted in each case. Error bars represent SD. Unpaired two-tailed *t*
616 test, ****$P<0.0001$.

617 **h, i,** Quantification of colocalization between immunostaining foci of Zip1 and Zip3 (**h**), and
618 Zip1 and Msh5 (**i**) from auxin-treated *ECM11-AID* nuclei represented in panels **e** and **f** with
619 auxin treated cells. Error bars represent SD.

620

621 **Methods**

622

623 **Data reporting**

624 No statistical methods were used to predetermine sample size. The experiments were not
625 randomized, and the investigators were not blinded to allocation during experiments. Blinding
626 was employed during outcome assessment for cytology experiments.
627
628 **Yeast Strains**
629 For full genotypes see **Supplementary Information Table 1**. The AID system [10] was optimized
630 for meiosis by replacing the promoter of the P_{ADH1}-*OsTIR1* cassette with the *CUP1* promoter[35].
631 C-terminal fusion of a minimal AID degron to targeted proteins was constructed using plasmid
632 pHyg-AID*-9Myc as template for PCR-mediated allele replacement [55]. To construct an internal
633 degron allele of *ZIP1,* AID degron sequences were inserted into plasmid pMPY-3xHA and
634 integrated after codon 700 via PCR epitope tagging [56]. Primers used to construct AID degron
635 alleles are listed in **Supplementary Information Table 2**. The estrogen-inducible *IN-NDT80*
636 *GAL4-ER* system has been described [57-59].
637
638 **Meiotic Time Courses and DNA Physical Assays**
639 Detailed protocols for meiotic time courses and DNA physical assays at the *HIS4::LEU2* locus
640 have been described [60]. At 6.5 h after induction of meiosis, CuSO4 (100 mM stock in dH2O)
641 was added for a final concentration of 50 μM to induce expression of P_{CUP1}-*OsTIR1* (encoding
642 the Tir1 E3 ligase) and cell cultures were split. At 7 h, estradiol (5 mM stock, Sigma E2758 in
643 ethanol) was added for a final concentration of 1 μM to both subcultures to induce *NDT80-IN*.
644 Simultaneously, auxin (3-indoleacetic acid, Sigma 13750, 2 M stock in DMSO) was added to
645 one subculture for a final concentration of 2 mM; an equivalent volume of DMSO was added to
646 the no-auxin control subculture. At 7.5 h, auxin was added again at 1 mM. To analyze the timing

647 and efficiency of meiotic divisions and sporulation, cells were fixed in 40% ethanol, 0.1 M
648 sorbitol, stained with DAPI, and ~200 cells were categorized for each time point. For imaging,
649 DAPI-stained cells were mounted in antifade (Vectashield, Vector Laboratories, Inc.) and digital
650 images captured using a Zeiss AxioPlan II microscope, Hamamatsu ORCA-ER CCD camera and
651 Volocity software.
652
653 **Chromosome spreading and immunofluorescence microscopy**
654 Cell samples were collected and processed for chromosome spreading and immunostaining
655 essentially as described [61]. Primary antibodies kindly provided by Akira Shinohara were chicken
656 anti-Red1 (1:500 dilution), rabbit anti-Msh5 (1:750), and rabbit anti-Zip3 (1:500); anti-Zip1
657 (1:400) was a gift from Scott Keeney; anti-myc (1:1000, Roche 11667149001) was used to
658 detect AID-9myc fused proteins. All primary antibodies were incubated overnight at room
659 temperature in 100 µl TBS/BSA buffer (10 mM Tris pH 7.5, 150 mM NaCl, 1% BSA).
660 Secondary antibodies anti-rabbit 568 (A11036 Molecular Probes, 1:1,000), anti-mouse 488
661 (A11029 Molecular Probes, 1:1,000), anti-rabbit 647 (A21245 Invitrogen), and anti-guinea pig
662 555 (A21435 Life Technologies) were incubated for 1 h at 37 °C. Coverslips were mounted with
663 Prolong Gold antifade reagent (Invitrogen, P36930). Digital images were captured using a Zeiss
664 Axioplan II microscope, Hamamatsu ORCA-ER CCD camera and analyzed using Volocity
665 software. Scatterplots were generated using the GraphPad program in Prism.
666
667 **Western Blot Analysis**
668 Whole cell extracts were prepared using a TCA extraction method, essentially as described [62].
669 Samples were analyzed by standard SDS-PAGE and Western blotting using the following

670 primary antibodies: anti-c-Myc (1:1000, Roche 11667149001), anti-HA (1:1000,
671 Sigma11583816001), Arp7 (1:10,000, Santa Cruz SC-8960), anti-Msh4 (1:500), and anti-Msh5
672 (1:500, Msh4 and Msh5 antibodies were a gift from Dr. Akira Shinohara). Secondary antibodies
673 (1:5000) were IRDye® 800CW Donkey anti-Mouse IgG (LI-COR 925-32212), IRDye® 680LT
674 Donkey anti-Goat IgG (LI-COR 925-68024), IRDye® 680LT Donkey anti-Rabbit IgG (LI-COR
675 925-68023) and IRDye® 800CW Donkey anti-Rabbit IgG (LI-COR 925-32213). Western blots
676 were imaged on an Odyssey Infrared Imager (LI-COR) and quantification of protein bands was
677 performed using Image Studio Lite Ver 4.0 software.
678
679 **Statistical analysis and Reproducibility**
680 Statistical analyses were performed using Prism (GraphPad software Inc.). For bar graphs and
681 scatter plots comparing two samples (aggregated from three or more replicate experiments),
682 unpaired *t*-tests were performed. For multiple comparisons, one-way ANOVA was performed
683 (Tukey or Dunnett tests, depending on the specific comparisons being made). For scatter plots
684 and bar graphs, error bars show the mean value with standard deviation. Western blots are
685 representative of at least three repeats (Figs. 1b, 4a 4b, Fig. 5c and 5d; and Extended Data Figs.
686 1a, 2a, 3a, 3c, 3e, 4a, 4g, 6a, 6f, 7a, 7g). Representative immunofluorescence images were
687 chosen from over 60 samples analyzed in each of at least three biological replicates (Figs. 1e, h,
688 2a, 3c, 2e, 2g, 3a, 4e 4g, 5a, 5e, 6a, 6c and 6e).
689
690 **Data availability**

691 Relevant data generated or analyzed during this study are included in this Article and its
692 Supplementary Information files. Biological materials are available from the corresponding
693 author.
694

695 55 Morawska, M. & Ulrich, H. D. An expanded tool kit for the auxin-inducible degron
696 system in budding yeast. *Yeast* **30**, 341-351 (2013). https://doi.org/10.1002/yea.2967
697 56 Schneider, B. L., Seufert, W., Steiner, B., Yang, Q. H. & Futcher, A. B. Use of
698 polymerase chain reaction epitope tagging for protein tagging in Saccharomyces
699 cerevisiae. *Yeast* **11**, 1265-1274 (1995). https://doi.org/10.1002/yea.320111306
700 57 Picard, D. Regulation of protein function through expression of chimaeric proteins. *Curr*
701 *Opin Biotechnol* **5**, 511-515 (1994).
702 58 Benjamin, K. R., Zhang, C., Shokat, K. M. & Herskowitz, I. Control of landmark events
703 in meiosis by the CDK Cdc28 and the meiosis-specific kinase Ime2. *Genes &*
704 *development* **17**, 1524-1539 (2003). https://doi.org/10.1101/gad.1101503
705 59 Carlile, T. M. & Amon, A. Meiosis I is established through division-specific translational
706 control of a cyclin. *Cell* **133**, 280-291 (2008). https://doi.org/S0092-8674(08)00283-3
707 60 Oh, S. D. *et al.* Stabilization and electrophoretic analysis of meiotic recombination
708 intermediates in Saccharomyces cerevisiae. *Methods in molecular biology* **557**, 209-234
709 (2009).
710 61 Grubb, J., Brown, M. S. & Bishop, D. K. Surface Spreading and Immunostaining of
711 Yeast Chromosomes. *J Vis Exp*, e53081 (2015). https://doi.org/10.3791/53081
712 62 Johnson, E. S. & Blobel, G. Cell cycle-regulated attachment of the ubiquitin-related
713 protein SUMO to the yeast septins. *The Journal of cell biology* **147**, 981-994 (1999).

714 63 Schmekel, K. & Daneholt, B. Evidence for close contact between recombination nodules
715 and the central element of the synaptonemal complex. *Chromosome Res* **6**, 155-159
716 (1998). https://doi.org/10.1023/a:1009295115033
717 64 Hollingsworth, N. M. & Gaglione, R. The meiotic-specific Mek1 kinase in budding yeast
718 regulates interhomolog recombination and coordinates meiotic progression with double-
719 strand break repair. *Curr Genet* **65**, 631-641 (2019). https://doi.org/10.1007/s00294-019-
720 00937-3
721

722 **End Notes**

723

724 **Acknowledgements** We thank A. Shinohara and S. Keeney for reagents; J. Matos for
725 communicating unpublished data; and members of the Hunter laboratory for support and
726 discussions. S.H. was supported by the predoctoral Training Program in Molecular and Cellular
727 Biology at UC Davis supported by NIH T32 training grant GM007377. This work was supported
728 by NIH NIGMS grant GM074223 to N.H. N.H. is an Investigator of the Howard Hughes
729 Medical Institute.

730

731 **Author contributions** S.M.T. and N.H. conceived the study and designed the experiments. S.H.,
732 R.B., J.E.M., J.K., M.P., E.N., N.L., C.M., H.L., and M.L. assisted with experiments and data
733 analysis. S.M.T and N.H. wrote the manuscript with inputs and edits from all authors.

734

735 **Competing interests** The authors declare no competing interests.

736

Additional Information

Supplementary Information is available for this paper.

Correspondence and requests for materials should be addressed to N.H.

Reprints and permissions information is available at www.nature.com/reprints.

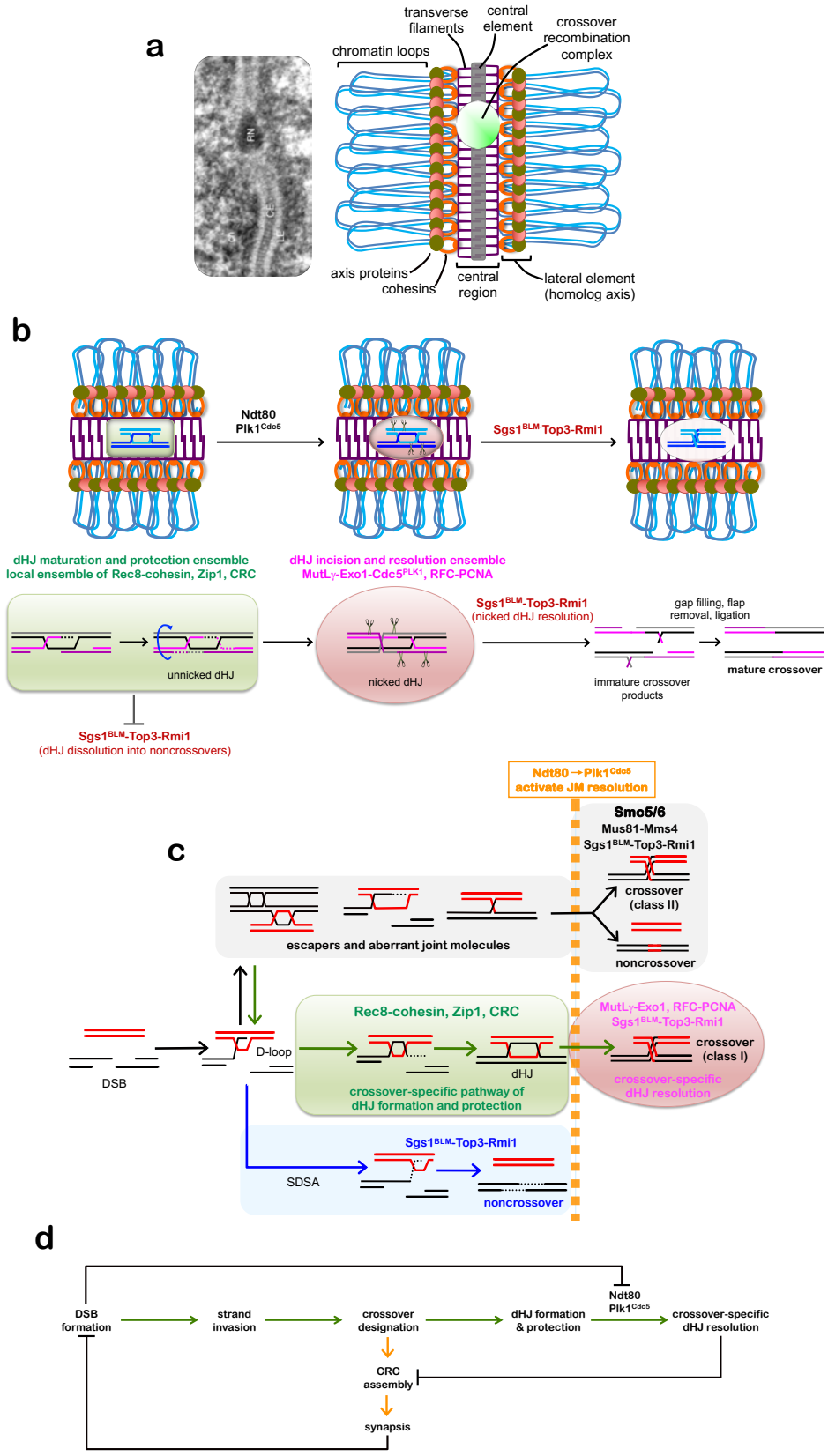
a
transverse filaments
central element
crossover recombination complex
chromatin loops
axis proteins cohesins
central region
lateral element (homolog axis)
b
Ndt80
Plk1Cdc5
Sgs1BLM-Top3-Rmi1
dHJ maturation and protection ensemble
local ensemble of Rec8-cohesin, Zip1, CRC
dHJ incision and resolution ensemble
MutLγ-Exo1-Cdc5PLK1, RFC-PCNA
unnicked dHJ
nicked dHJ
Sgs1BLM-Top3-Rmi1
(nicked dHJ resolution)
gap filling, flap removal, ligation
immature crossover products
mature crossover
Sgs1BLM-Top3-Rmi1
(dHJ dissolution into noncrossovers)
c
Ndt80 → Plk1Cdc5
activate JM resolution
Smc5/6
Mus81-Mms4
Sgs1BLM-Top3-Rmi1
crossover (class II)
escapers and aberrant joint molecules
noncrossover
Rec8-cohesin, Zip1, CRC
MutLγ-Exo1, RFC-PCNA
Sgs1BLM-Top3-Rmi1
crossover (class I)
DSB
D-loop
dHJ
crossover-specific pathway of dHJ formation and protection
crossover-specific dHJ resolution
Sgs1BLM-Top3-Rmi1
SDSA
noncrossover
d
DSB formation
strand invasion
crossover designation
dHJ formation & protection
Ndt80
Plk1Cdc5
crossover-specific dHJ resolution
CRC assembly
synapsis

743

744 **Extended Data Fig. 1. Summary and Model.**

745 **a,** Electron micrograph of SC from *Blaps cribrosa*[63] and schematic highlighting the key features
746 of pachytene-stage chromosomes. Ch, chromatin; LE, lateral element; CE, central element, RN,
747 recombination nodule (the site of a crossover recombination complex, CRC).

748 **b,** Rec8-cohesin, Zip1, and CRCs constitute local dHJ maturation and protection ensembles that
749 facilitates dHJ formation and protects unnicked dHJs from being dissolved into non-crossovers
750 by the BLM/STR complex. dHJ protection must be maintained until Ndt80-dependent expression
751 of polo-like kinase $Plk1^{Cdc5}$ triggers crossover-specific resolution via a two-step mechanism: (i)
752 strand-specific nicking of dHJs by the MutLγ endonuclease and associated factors[4]; (ii)
753 resolution of nicked dHJs by the BLM/STR complex. Placement of the nicks, on both sides of
754 the two Holliday junctions but distal to the exchange points, specifies a crossover outcome.

755 **c,** Pathways of joint-molecule resolution during meiotic recombination. Resected DSB ends
756 undergo homology search and DNA strand exchange to form nascent displacement loops (D-
757 loops) as common precursors to all pathways. Non-crossover fated D-loops are unwound by
758 BLM/STR to effect synthesis-dependent strand annealing (SDSA), independently of $Plk1^{Cdc5}$. D-
759 loops that are designated a crossover fate mature into dHJs. In this class-I pathway, $Plk1^{Cdc5}$
760 triggers two-step crossover-specific resolution as described in **b**. All other joint-molecule
761 structures are resolved via a Smc5/6-dependent pathway that is also dependent on $Plk1^{Cdc5}$ and
762 yields class-II crossovers and non-crossovers.

763 **d,** Dependencies that help ensure crossing over between homologs. At designated crossover
764 sites, CRC assembly promotes and maintains homolog synapsis and dHJs. In turn, synapsis
765 globally attenuates DSB formation[53], thereby diminishing the DNA-damage kinase signaling that

766 inhibits Ndt80 activity[64]. Ndt80-dependent expression of Plk1^{Cdc5} then activates crossover-

767 specific dHJ resolution, CRCs disassemble, and desynapsis ensues.

768

769

770

771

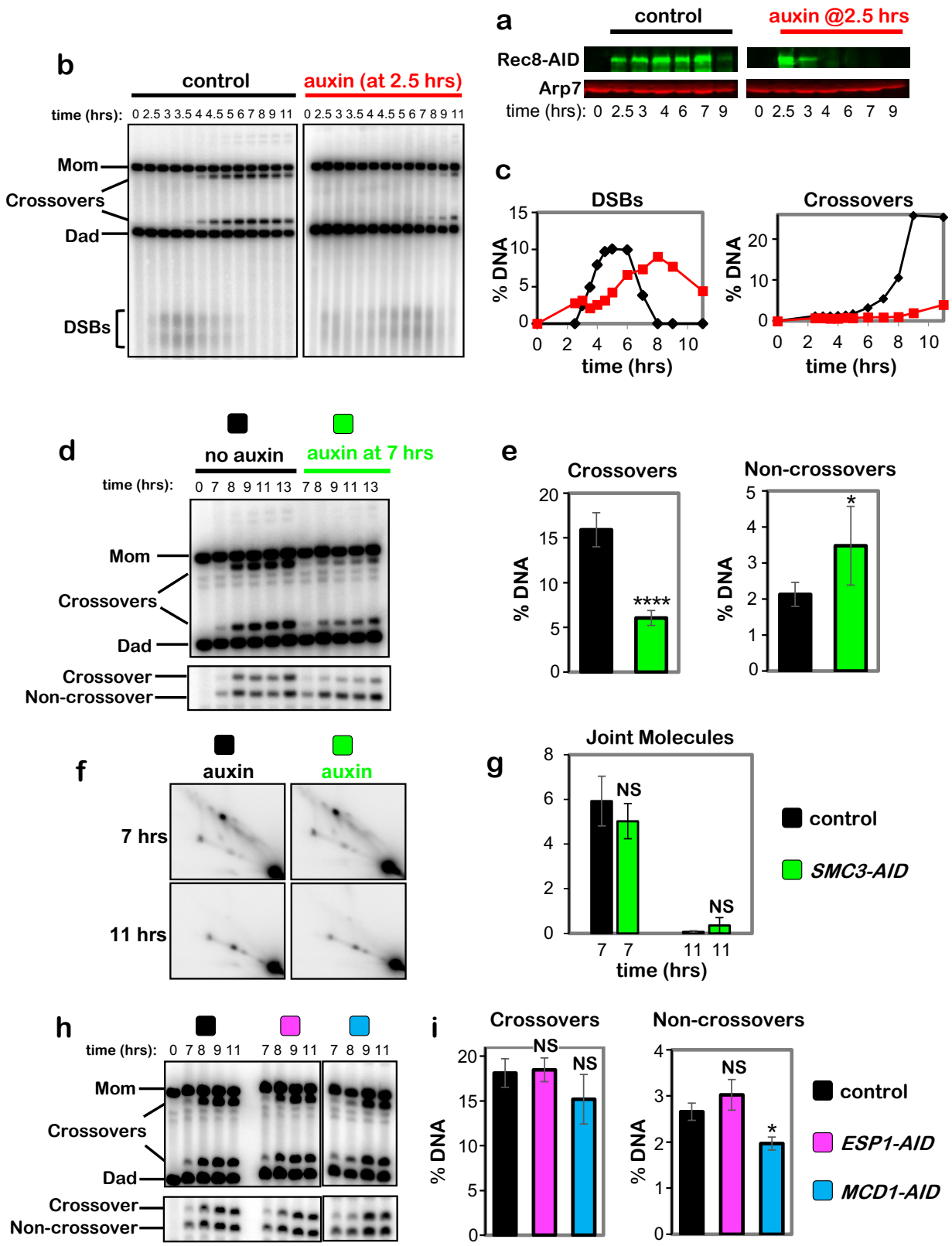
a
control
auxin @2.5 hrs
Rec8-AID
Arp7
time (hrs): 0 2.5 3 4 6 7 9
0 2.5 3 4 6 7 9
b
control
auxin (at 2.5 hrs)
time (hrs): 0 2.5 3 3.5 4 4.5 5 6 7 8 9 11
0 2.5 3 3.5 4 4.5 5 6 7 8 9 11
Mom
Crossovers
Dad
DSBs
c
DSBs
Crossovers
% DNA
time (hrs)
d
no auxin
auxin at 7 hrs
time (hrs): 0 7 8 9 11 13 7 8 9 11 13
Mom
Crossovers
Dad
Crossover
Non-crossover
e
Crossovers
Non-crossovers
% DNA
****
*
f
auxin
auxin
7 hrs
11 hrs
g
Joint Molecules
NS
NS
7 7 11 11
time (hrs)
control
SMC3-AID
h
time (hrs): 0 7 8 9 11 7 8 9 11 7 8 9 11
Mom
Crossovers
Dad
Crossover
Non-crossover
i
Crossovers
Non-crossovers
% DNA
NS
NS
NS
*
control
ESP1-AID
MCD1-AID

772

773 **Extended Data Fig. 2. Early functions of Rec8 and roles of Smc3, Kleisin Mdc1^{Rad21,} and**
774 **Separase Esp1 in crossover-specific dHJ resolution.**
775 **a,** Western analysis of early Rec8-AID degradation following addition of auxin at 2.5 hrs.
776 **b,** 1D-gel Southern analysis of DSBs and crossovers following early degradation of Rec8-AID.
777 **c,** Quantification of the DSB and crossover level from the Southern blot shown in C.
778 **d,** Representative 1D-gel Southern analysis of crossover (upper panel) and non-crossover (lower
779 panel) formation from *SMC3-AID* subcultures with or without auxin.
780 **e,** Quantification of final levels of crossovers and non-crossovers at 13 hrs from *SMC3-AID*
781 subcultures with or without auxin (mean ± SD, 4 independent experiments, ****P<0.0001, NS,
782 not significant P=0.0561, two-tailed unpaired t-test).
783 **f,** Representative 2D gel Southern analysis of joint molecules from *SMC3-AID* subcultures with
784 or without auxin, before and after release from arrest at 7 and 11 hrs, respectively.
785 **g,** Quantification of total joint molecule levels from experiments represented in panel **f** (mean ±
786 SD, 3 independent experiments, NS, not significant, P=0.3167 for levels at 7hrs; NS, not
787 significant, P >0.9999 for levels at 11hrs; two-tailed unpaired t-test).
788 **h,** Representative 1D-gel Southern analysis of crossover (upper panel) and non-crossover (lower
789 panel) formation in control, *ESP1-AID* (with auxin) or *MCD1-AID* (with auxin) strains.
790 **i,** Final levels of crossovers and non-crossovers at 11 hrs from the indicated strains (mean ± SD,
791 3 independent experiments, *P=0.0146; NS, not significant, P=0.9610 (crossovers, control vs.
792 *ESP1-AID*), P=0.1793 (crossovers, control vs. *MCD1-AID*), P=0.2073 (noncrossovers, control
793 vs. *ESP1-AID*), Dunnett's multiple comparisons test, control).
794
795

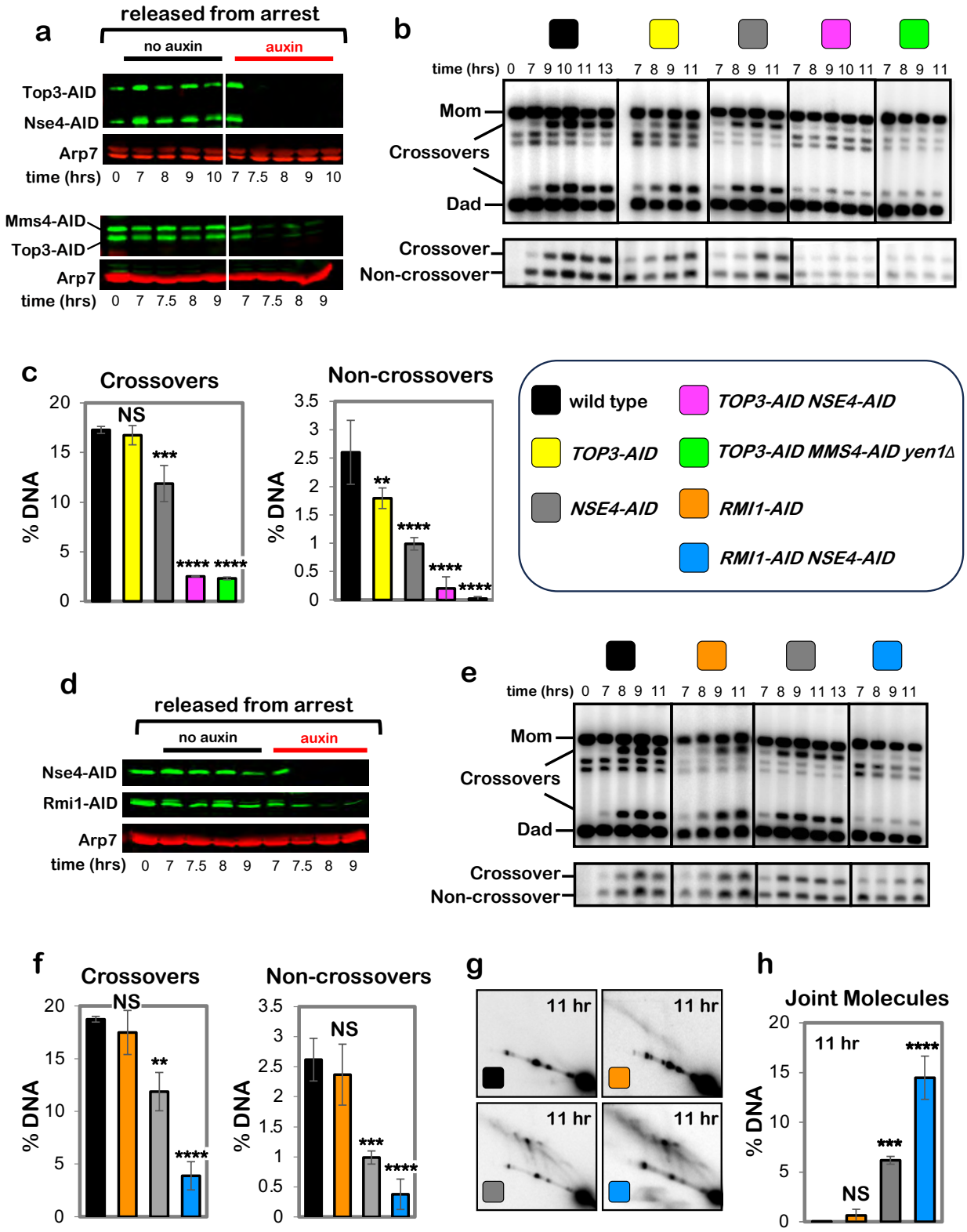
a
released from arrest
no auxin
auxin
Top3-AID
Nse4-AID
Arp7
time (hrs) 0 7 8 9 10 7 7.5 8 9 10
Mms4-AID
Top3-AID
Arp7
time (hrs) 0 7 7.5 8 9 7 7.5 8 9
b
time (hrs) 0 7 9 10 11 13 7 8 9 11 7 8 9 11 7 8 9 10 11 7 8 9 11
Mom
Crossovers
Dad
Crossover
Non-crossover
c
Crossovers
% DNA
NS
***
****
****
Non-crossovers
% DNA
**
****
****
****
wild type
TOP3-AID
NSE4-AID
TOP3-AID NSE4-AID
TOP3-AID MMS4-AID yen1Δ
RMI1-AID
RMI1-AID NSE4-AID
d
released from arrest
no auxin
auxin
Nse4-AID
Rmi1-AID
Arp7
time (hrs) 0 7 7.5 8 9 7 7.5 8 9
e
time (hrs) 0 7 8 9 11 7 8 9 11 7 8 9 11 13 7 8 9 11
Mom
Crossovers
Dad
Crossover
Non-crossover
f
Crossovers
% DNA
NS
**
****
Non-crossovers
% DNA
NS
***
****
g
11 hr
11 hr
11 hr
11 hr
h
Joint Molecules
% DNA
11 hr
NS
***
****

796

797 **Extended Data Fig. 3. Sgs1-Top3-Rmi1 and Smc5/6 mediate essentially all joint-molecule**
798 **resolution.**
799 **a**, Western blot analysis of Top3-AID and Nse4-AID co-degradation in cells released from
800 pachytene-arrest and addition of auxin at 7 hours.
801 **b**, Representative 1D-gel Southern analysis of crossover (upper panel) and non-crossover (lower
802 panel) formation in control, *TOP3-AID* (with auxin), *NSE4-AID* (with auxin), *TOP3-AID NSE4-*
803 *AID* (with auxin) and *TOP3-AID NSE4-AID yen1Δ* (with auxin) following release from
804 pachytene arrest.
805 **c**, Final levels of crossovers and non-crossovers at 11 hrs from experiments represented in **b**
806 (mean ± SD). Statistical comparisons with control: ****P<0.0001, ***P=0.0003, NS, not
807 significant, P=0.3101 (crossovers, *TOP3-AID* vs. control), P=0.003 (crossovers, *NSE4-AID* vs.
808 control), P= 0.0029 (non-crossovers *TOP3-AID* vs. control), Dunnett's multiple comparisons
809 test. Number of experiments: control: control: n=3, *TOP3-AID*: n=3, *NSE4-AID*: n=3, *TOP3-AID*
810 *NSE4-AID*: n=3 and *TOP3-AID NSE4-AID yen1Δ*, n=2.
811 **d**, Western blot analysis of RMI1-AID and Nse4-AID co-degradation in cells released from
812 pachytene-arrest and addition of auxin at 7 hours.
813 **e**, Representative 1D-gel Southern analysis of crossover (upper panel) and non-crossover (lower
814 panel) formation in control, *RMI1-AID* (with auxin), *NSE4-AID* (with auxin) and *RMI1-AID*
815 *NSE4-AID* (with auxin) following release from pachytene arrest.
816 **f,** Final levels of crossovers and non-crossovers at 11 hrs from experiments represented in **b**
817 (mean ± SD). Statistical comparisons with control: ****P<0.0001, ***P=0.0002, **P=0.0016,
818 NS, not significant, P=0.9928 (crossovers, *RMI1-AID* vs. control), P=0.7036 (non-crossovers

819 *RMI1-AID* vs. control), Dunnett's multiple comparisons test. Number of experiments: control:

820 control: n=4, *RMI1-AID*: n=2, *NSE4-AID*: n=4 and *RMI1-AID NSE4-AID*: n=3.

821 **g**, Representative 2D gel Southern analysis of joint molecules from control, *RMI1-AID, NSE4-*

822 *AID and RMI1-AID NSE4-AID* subcultures with auxin after release from arrest at 11 hrs.

823 **h**, Quantification of total joint molecule levels from experiments represented in panel **g** (mean ±

824 SD), NS, not significant, P=0.8596, ***P=0.0002, ****P<0.0001, Dunnett's multiple

825 comparisons test. control: n=3, *RMI1-AID*: n=3, *NSE4-AID*: n=3 and *RMI1-AID NSE4-AID*: n=3.

826

827

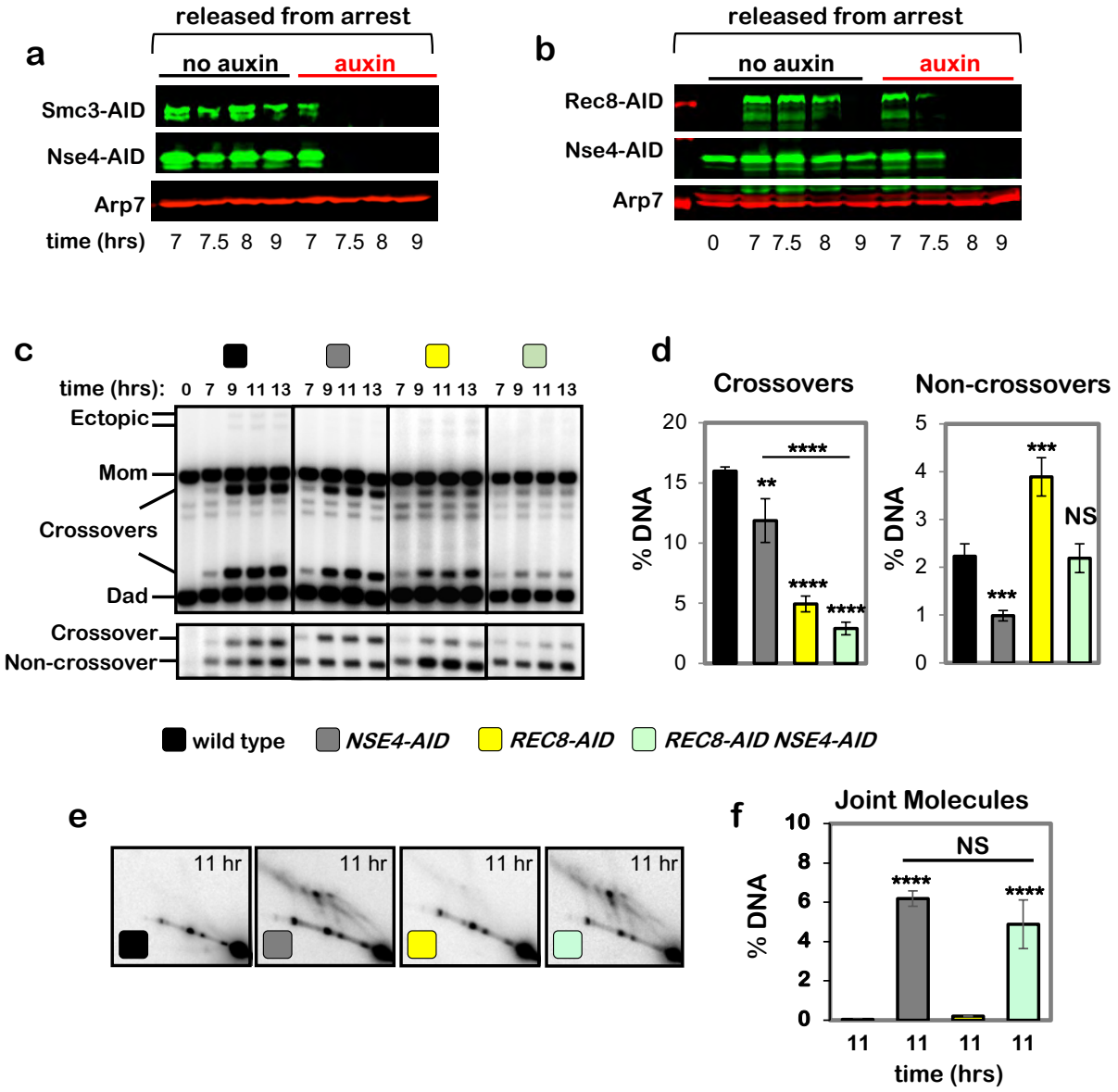

Extended Data Fig. 4. Cohesin and the Smc5/6 complex act in parallel pathways of joint-molecule resolution.

a, Western blot images of Smc3-AID Nse4-AID co-degradation following auxin addition at 7 hours (corresponds to experiments in **Fig2. e–g**). Arp7 is a loading control.

833 **b,** Western blot images of Rec8-AID Nse4-AID co-degradation following auxin addition at 7
834 hours.
835 **c,** Representative 1D-gel Southern analysis of crossover (upper panel) and non-crossover (lower
836 panel) formation in control, *NSE4-AID* (with auxin), *REC8-AID* (with auxin), and *NSE4-AID*
837 *REC8-AID* (with auxin) strains.
838 **d,** Final levels of crossovers and non-crossovers at 11 hrs from experiments represented in **c**
839 (mean ± SD, 3 independent experiments). Statistical comparisons with control unless indicated.
840 Dunnett's multiple comparisons test, ****P<0.0001, **P=0.0049 (*NSE4-AID* vs. control),
841 ***P=0.0002 (*REC8-AID* vs. control), ***P=0.0022 (*NSE4-AID* vs. control), NS, not significant
842 P=0.9955).
843 **e,** Representative Southern blot 2D gel images at 11 hours from no auxin control, *NSE4-AID*
844 (with auxin), *REC8-AID* (with auxin) and *REC8-AID NSE4-AID* (with auxin).
845 **f,** Quantification of total joint-molecule levels from the experiments represented in **e** (mean ±
846 SD, 3 independent experiments). NS, not significant, P=0.3320 Tukey's multiple comparison
847 test.
848
849

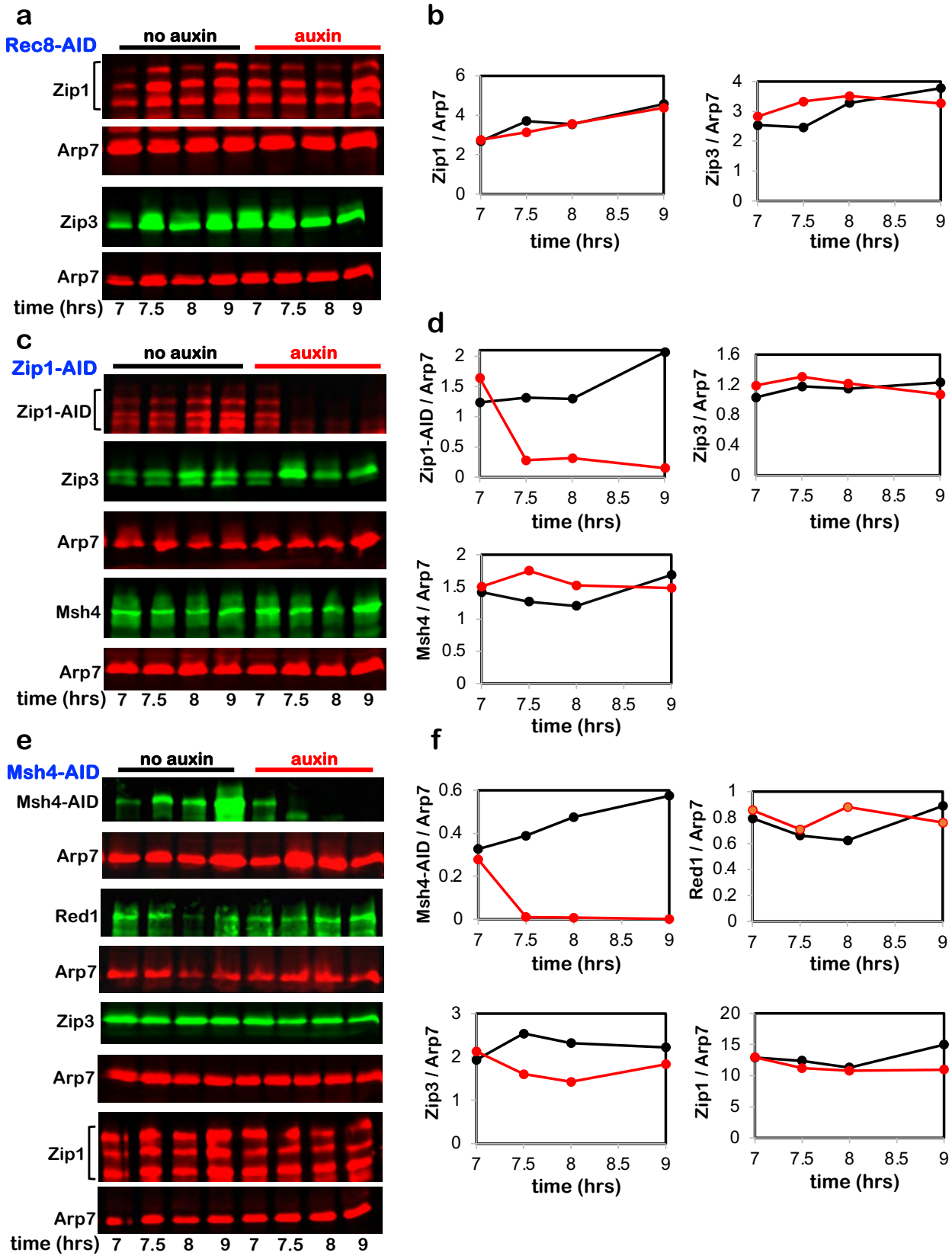
a
Rec8-AID
no auxin
auxin
Zip1
Arp7
Zip3
Arp7
time (hrs) 7 7.5 8 9 7 7.5 8 9
b
Zip1 / Arp7
Zip3 / Arp7
time (hrs)
c
Zip1-AID
no auxin
auxin
Zip1-AID
Zip3
Arp7
Msh4
Arp7
time (hrs) 7 7.5 8 9 7 7.5 8 9
d
Zip1-AID / Arp7
Zip3 / Arp7
Msh4 / Arp7
time (hrs)
e
Msh4-AID
no auxin
auxin
Msh4-AID
Arp7
Red1
Arp7
Zip3
Arp7
Zip1
Arp7
time (hrs) 7 7.5 8 9 7 7.5 8 9
f
Msh4-AID / Arp7
Red1 / Arp7
Zip3 / Arp7
Zip1 / Arp7
time (hrs)

850

851 **Extended Data Fig. 5. Targeted degradation does not cause off-target effects.**

852 **a,** Representative Western blot analysis of Zip1 and Zip3 with or without Rec8-AID degradation

853 following auxin addition at 7 hours.

854 **b,** Quantification of Zip1 and Zip3 level from the experiments shown in **a**.

855 **c,** Representative Western blot analysis of Zip3 and Msh4 with or without Zip1-AID degradation

856 following auxin addition at 7 hours.

857 **d,** Quantification of Zip1-AID, Zip3, and Msh4 levels from the experiments shown in **c**.

858 **e,** Representative Western blot analysis of Red1, Zip3, and Zip1 with or without Msh4-AID

859 degradation following auxin addition at 7 hours.

860 **F,** Quantification of Msh4-AID, Red1, Zip3, and Zip1 level from the experiments shown in **e**.

861 Arp7 is the loading control in all experiments.

862

863

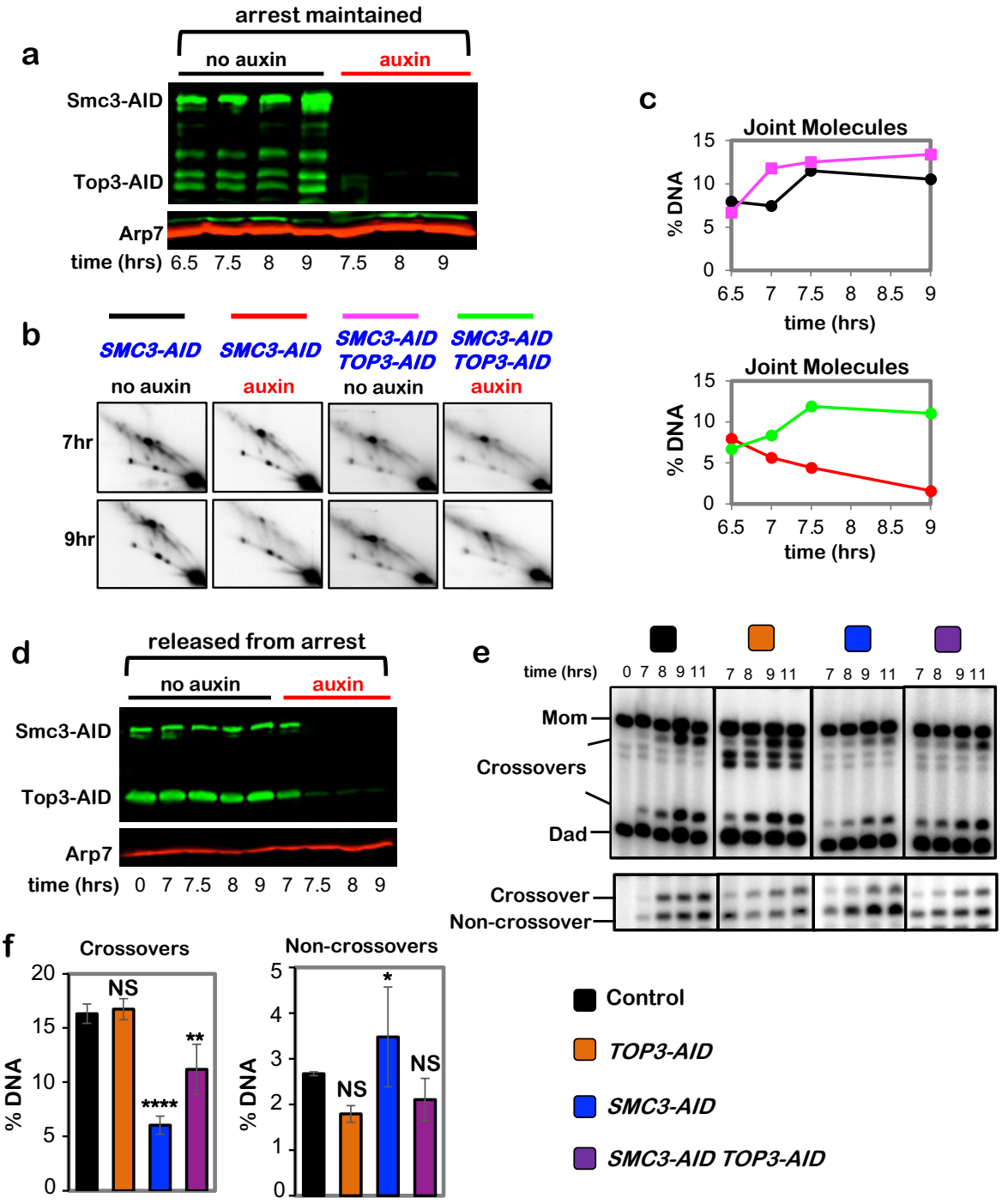
a
arrest maintained
no auxin
auxin
Smc3-AID
Top3-AID
Arp7
time (hrs) 6.5 7.5 8 9 7.5 8 9
b
SMC3-AID
SMC3-AID
SMC3-AID TOP3-AID
SMC3-AID TOP3-AID
no auxin
auxin
no auxin
auxin
7hr
9hr
c
Joint Molecules
% DNA
time (hrs)
Joint Molecules
% DNA
time (hrs)
d
released from arrest
no auxin
auxin
Smc3-AID
Top3-AID
Arp7
time (hrs) 0 7 7.5 8 9 7 7.5 8 9
e
time (hrs) 0 7 8 9 11 7 8 9 11 7 8 9 11 7 8 9 11
Mom
Crossovers
Dad
Crossover
Non-crossover
f
Crossovers
% DNA
NS
****
**
Non-crossovers
% DNA
NS
*
NS
Control
TOP3-AID
SMC3-AID
SMC3-AID TOP3-AID

864

865 **Extended Data Fig. 6. Cohesin protects dHJs from dissolution by the BLM/STR complex.**

866 **a,** Western blot analysis of Smc3-AID and Top3-AID co-degradation in pachytene-arrested cells

867 following the addition of auxin at 7 hours. Arp7 is a loading control.

868 **b,** Representative 2D gel Southern analysis of joint molecules from subcultures of pachytene

869 arrested *SMC3-AID* and *SMC3-AID TOP3-AID* strains, with or without the addition of auxin.

870 **c,** Quantification of total joint molecules from experiments shown in **b**.

871 **d,** Western blot analysis of Smc3-AID and Top3-AID co-degradation in cells released from

872 pachytene-arrest and addition of auxin at 7 hours. Arp7 is used as loading control.

873 **e,** Representative 1D-gel Southern analysis of crossover (upper panel) and non-crossover (lower

874 panel) formation in control, *TOP3-AID* (with auxin), *SMC3-AID* (with auxin) and *SMC3-AID*

875 *TOP3-AID* (with auxin) following release from pachytene arrest.

876 **f,** Final levels of crossovers and non-crossovers at 11 hrs from experiments represented in **g**

877 (mean ± SD, 3 (*SMC3-AID* and *TOP3-AID SMC3-AID*) or 4 (*TOP3-AID* and *SMC3-AID*)

878 independent experiments). Statistical comparisons with control: ****P<0.0001, ** P= 0.0038,

879 NS, not significant, P=0.9876 (crossovers, *TOP3-AID* vs. control), *P=0.0423. NS, not

880 significant, P=0.8549 (non-crossovers, *TOP3-AID* vs. control), NS, not significant, P >0.9999

881 (non-crossovers, *TOP3-AID SMC3-AID* vs. control), Dunnett's multiple comparisons test.

882

883

884

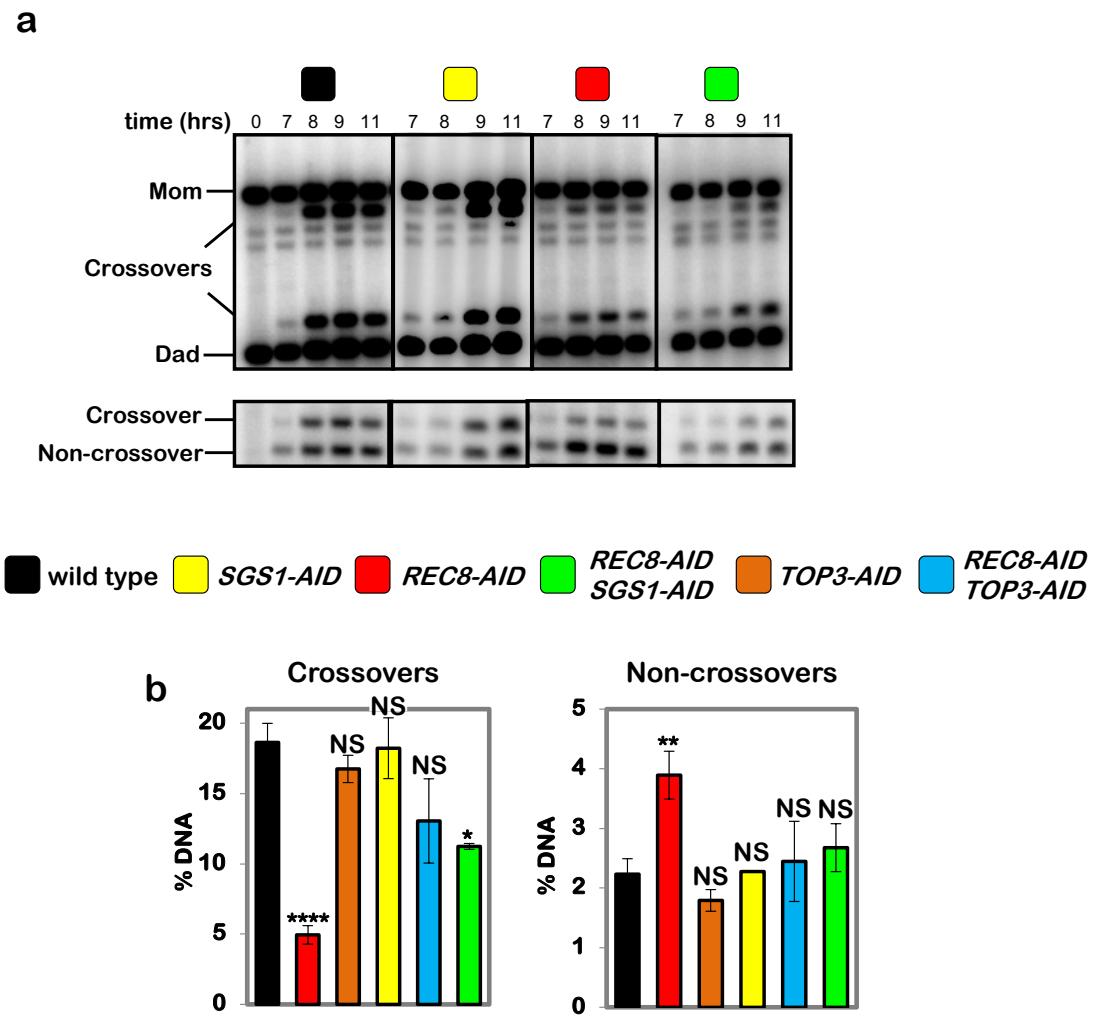

885

886

887 **Extended Data Fig. 7. Sgs1-AID degradation partially suppresses the crossover defect**

888 **resulting from degradation of Rec8-AID.**

889 **a,** Representative 1D-gel Southern analysis of crossover (upper panel) and non-crossover (lower

890 panel) formation following release from pachytene arrest in control, *SGS1-AID* (with auxin),

891 *REC8-AID* (with auxin), *REC8-AID SGS1-AID* (with auxin).

892 **b,** Final levels of crossovers and non-crossovers at 11 hrs from the indicated strains (mean ±

893 SD). Data for *TOP3-AID* and *REC8-AID TOP3-AID* from **Fig. 5e** are shown for comparison.

894 ****P<0.0001, *P=0.0162, **P=0.0012; NS, not significant. Crossovers: P=0.9378 (*TOP3-AID*

895 vs. control), P=0.3345 (*SGS1-AID* vs. control), P=0.1490 (*REC8-AID TOP3-AID* vs. control);

896 Non-crossovers: P=0.4759 (*TOP3-AID* vs. control), P>0.9999 (*SGS1-AID* vs. control), P=

897 0.9465 (*REC8-AID TOP3-AID* vs. control), P=0.5646 (*REC8-AID SGS1-AID* vs. control),

898 Dunnett's multiple comparisons tests. Number of experiments: control n=3, *TOP3-AID* n=3,

899 *SGS1-AID* n=2, *REC8-AID* n=3, REC8-AID SGS1-AID n=2, *TOP3-AID REC8-AID* n=2.

900

901

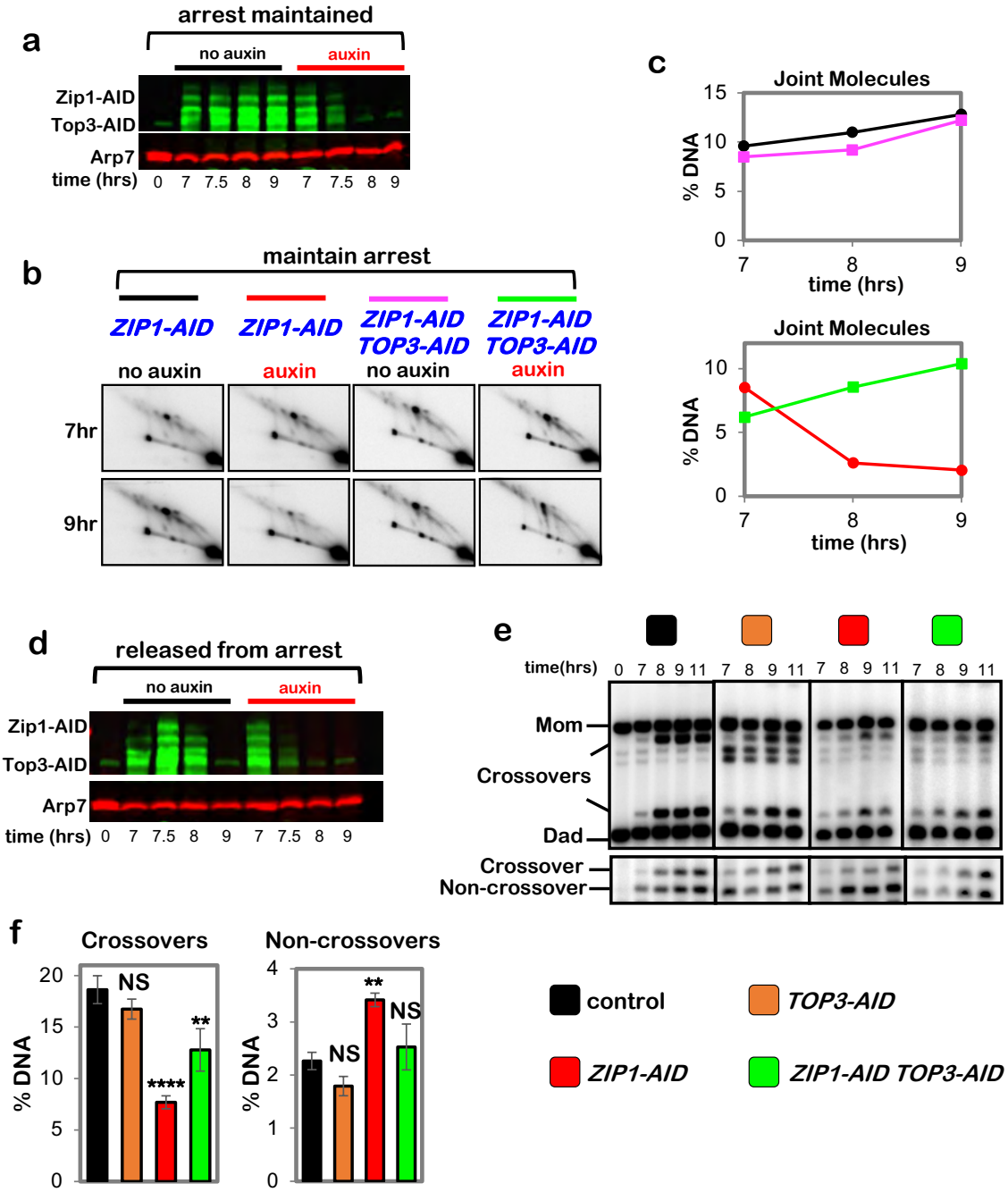

Extended Data Fig. 8. Zip1 protects double-Holliday junctions from aberrant resolution mediated by the BLM/STR complex.

a, Western blot analysis of Zip1-AID and Top3-AID co-degradation in pachytene-arrested cells following the addition of auxin at 7 hours. Arp7 is a loading control.

908 **b,** Representative 2D gel Southern analysis of joint molecules from subcultures of pachytene
909 arrested *ZIP1-AID* and *ZIP1-AID TOP3-AID* strains, with or without the addition of auxin.
910 **c,** Quantification of total joint molecules from experiments shown in **b**.
911 **d,** Western blot analysis of Zip1-AID and Top3-AID co-degradation in cells released from
912 pachytene-arrest and addition of auxin at 7 hours.
913 **e,** Representative 1D-gel Southern analysis of crossover (upper panel) and non-crossover (lower
914 panel) formation in control, *TOP3-AID* (with auxin), *ZIP1-AID* (with auxin) and *ZIP1-AID TOP3-*
915 *AID* (with auxin) following release from pachytene arrest.
916 **f,** Final levels of crossovers and non-crossovers at 11 hrs from experiments represented in **g**
917 (mean ± SD). Statistical comparisons with control: ****P<0.0001, **P=0.0022, NS, not
918 significant. P=0.1011 (crossovers *TOP3-AID* vs. control), P=0.1104 (non-crossovers *TOP3-AID*
919 vs. control), P=0.5171 (non-crossovers *ZIP1-AID TOP3-AID* vs. control), Dunnett's multiple
920 comparisons tests. Number of experiments: control: n=3, *TOP3-AID*: n=3, *ZIP1-AID*: n=2,
921 *ZIP1-AID TOP3-AID*: n=2.
922
923

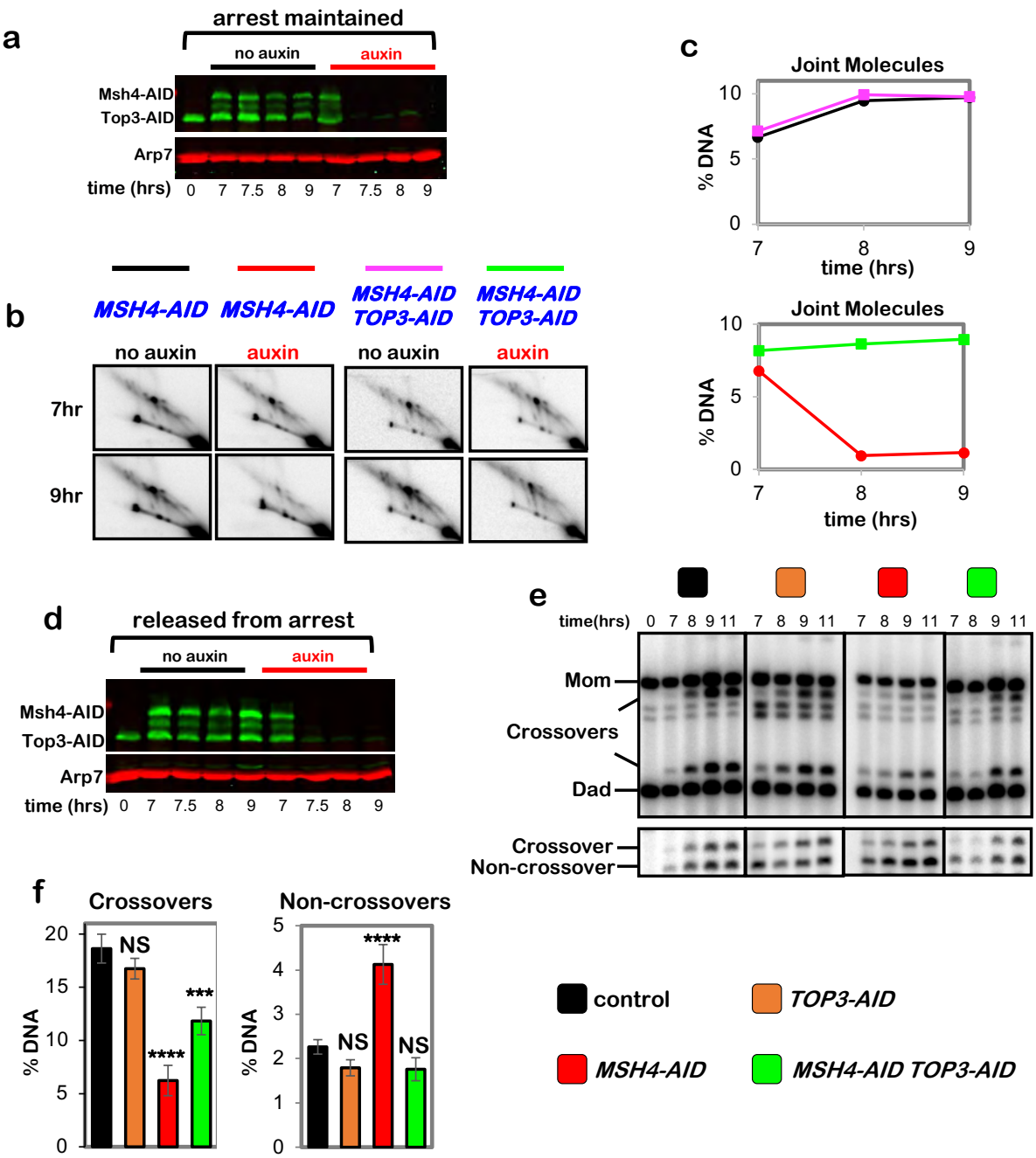

Extended Data Fig. 9. MutSγ protects double-Holliday junctions from aberrant resolution mediated by the BLM/STR complex.

a, Western blot analysis of Msh4-AID and Top3-AID co-degradation in pachytene-arrested cells following the addition of auxin at 7 hours. Arp7 is a loading control.

930 **b,** Representative 2D gel Southern analysis of joint molecules from subcultures of pachytene
931 arrested *MSH4-AID* and *MSH4-AID TOP3-AID* strains, with or without the addition of auxin.
932 **c,** Quantification of total joint molecules from experiments shown in **b**.
933 **d,** Representative 1D gel Southern analysis of non-crossover formation from subcultures of
934 pachytene arrested *MSH4-AID* and *MSH4-AID TOP3-AID* strains, with or without the addition
935 of auxin (the same experiments analyzed in panel **b**).
936 **e,** Quantification of non-crossovers from pachytene arrested *MSH4-AID* (red) and *MSH4-AID*
937 *TOP3-AID* (green) strains following the addition of auxin.
938 **f,** Western blot analysis of Msh4-AID and Top3-AID co-degradation in cells released from
939 pachytene-arrest and addition of auxin at 7 hours.
940 **g,** Representative 1D-gel Southern analysis of crossover (upper panel) and non-crossover (lower
941 panel) formation in control, *TOP3-AID* (with auxin), *MSH4-AID* (with auxin) and *MSH4-AID*
942 *TOP3-AID* (with auxin) following release from pachytene arrest.
943 **h,** Final levels of crossovers and non-crossovers at 11 hrs from experiments represented in **g**
944 (mean ± SD). Statistical comparisons with control: ****$P<0.0001$, ***$P=0.0003$, NS, not
945 significant, $P>0.9999$ (crossovers, *TOP3-AID* vs. control), $P=0.0821$ (non-crossovers *TOP3-AID*
946 vs. control), $P=0.0638$ (non-crossovers *TOP3-AID MSH4-AID* vs. control), Dunnett's multiple
947 comparisons test. Number of experiments: control: control: n=6, *TOP3-AID*: n=3, *MSH4-AID*:
948 n=6, *TOP3-AID MSH4-AID*: n=3.
949
950
951
952

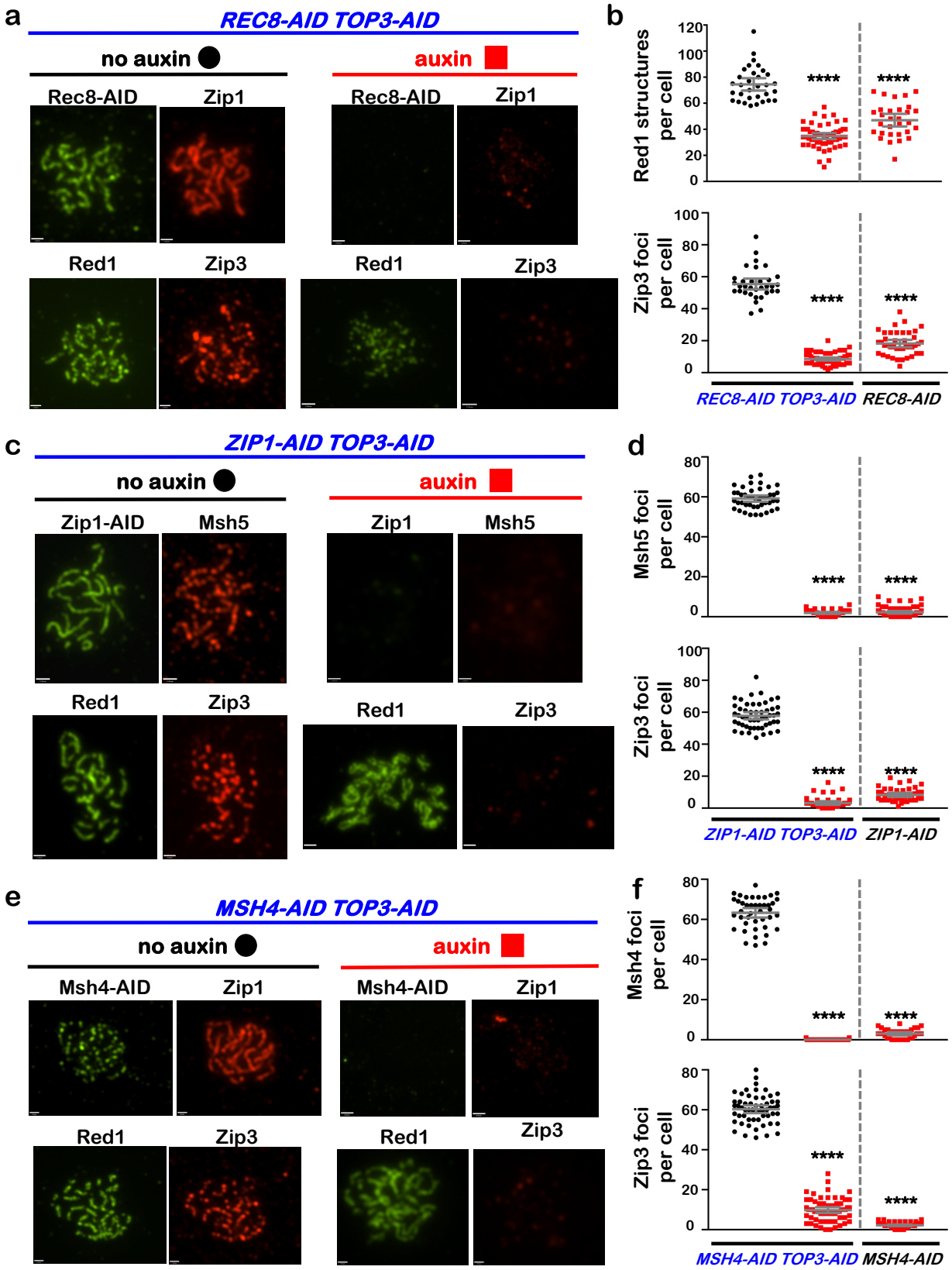
a
REC8-AID TOP3-AID
no auxin
auxin
Rec8-AID
Zip1
Red1
Zip3
b
Red1 structures per cell
Zip3 foci per cell
****
REC8-AID TOP3-AID
REC8-AID
c
ZIP1-AID TOP3-AID
Zip1-AID
Msh5
d
Msh5 foci per cell
ZIP1-AID TOP3-AID
ZIP1-AID
e
MSH4-AID TOP3-AID
Msh4-AID
f
Msh4 foci per cell
MSH4-AID TOP3-AID
MSH4-AID

953

954 **Extended Data Fig. 10. Stabilizing dHJs in pachytene does not bypass interdependence**
955 **between cohesin, synapsis, and crossover recombination complexes**
956 **a,** Representative images of surface-spread meiotic nuclei from pachytene-arrested *REC8-AID*
957 *TOP3-AID* cells sampled 1 hr after the addition of auxin or DMSO vehicle at 7 hrs, and
958 immunostained for the indicated markers.
959 **b,** Quantification of Red1 and Zip3 immunostaining structures from the *REC8-AID TOP3-AID*
960 experiments represented in panel **a**, and comparison with corresponding data from *REC8-AID*
961 (from **Fig. 3b**).
962 **c,** Representative images of surface-spread meiotic nuclei from pachytene-arrested *ZIP1-AID*
963 *TOP3-AID* cells sampled 1 hr after the addition of auxin or DMSO vehicle at 7 hrs, and
964 immunostained for the indicated markers.
965 **d,** Quantification of Msh5 and Zip3 immunostaining foci from the experiments represented in
966 panel **c**, and comparison with corresponding data from *ZIP1-AID* (from **Fig. 4f**).
967 **e,** Representative images of surface-spread meiotic nuclei from pachytene-arrested *MSH4-AID*
968 *TOP3-AID* cells sampled 1 hr after the addition of auxin or DMSO vehicle at 7 hrs, and
969 immunostained for the indicated markers.
970 **f,** Quantification of Msh4 and Zip3 immunostaining foci from the experiments represented in
971 panel **e**, and comparison with corresponding data from *MSH4-AID* (from **Fig. 4h**).
972 Scale bars = 1 μm. Error bars represent SD. 40-60 nuclei were counted in each case. Unpaired
973 two-tailed *t* test, ****$P<0.0001$.
974
975